10. VOLTAGE CLAMPING OF EXCITABLE MEMBRANES

By Francisco Bezanilla, Julio Vergara, and Robert E. Taylor

10.1. Introduction

"Animal electricity" was discussed by Galvani in his *Commentary* of 1791 (English translation by Green[1]) and, as pointed out by Hodgkin[2] in his Sherrington Lecture, Volta, in 1800, compared his battery to the stack of plates in the electric fish. Thus the observation that animals produce or respond to electrical changes is very old. Most of the early work on excitable cells, such as nerve and muscle,[3–5] was done by applying known currents and measuring the electrical or mechanical responses. Typically, no (or a very small) response occurs if the stimulus is below "threshold," and when the system "fires," one loses control. The excitability resides in a surface membrane in the form of channels which are embedded in a lipid bilayer with a rather large capacitance (about 1.0 μF/cm^2). They are either open or closed, and the proportion of the time any one is open is potential dependent.

To see why control of the membrane voltage, or voltage clamping, is so important in the study of excitable membranes, consider the components of the current I_m through a membrane. There are two broad categories: current carried by ions and dielectric, or displacement, currents. For frequencies above a few kilocycles per second (kHz), the capacitance C_m of the membrane is almost independent of potential V_m,[6,7] so the capacitative current is $C_m\, dV_m/dt$. There is a small component of capacitative current, which is potential and time dependent, associated with the movement of

[1] R. M. Green, English translation of Luigi Galvani's "de Viribus Electricitatis in motu musculari commentarius" with introduction and other translations. Licht, Cambridge, Massachusetts, 1953.

[2] A. L. Hodgkin, "The Conduction of the Nervous Impulse." Thomas, Springfield, Illinois, 1964.

[3] B. Katz, "Electric Excitation of Nerve." Oxford Univ. Press, London and New York, 1939.

[4] A. L. Hodgkin and W. A. H. Rushton, *Proc. R. Soc. London, Ser. B* **133**, 444 (1946).

[5] R. E. Taylor, *Phys. Tech. Biol. Res.* **6**, 219 (1963).

[6] H. J. Curtis and K. S. Cole, *J. Gen. Physiol.* **21**, 757 (1938).

[7] K. S. Cole, "Membranes, Ions, and Impulses." Univ. of California Press, Berkeley, 1972.

METHODS OF EXPERIMENTAL PHYSICS, VOL. 20

ISBN 0-12-475962-9

charge within the membrane responsible for the initiation of the voltage-dependent ionic conductance changes which will be considered in Section 10.3.6.3. It is sometimes necessary to include the fact that the capacitance is lossy, probably because of the loss in the penetrating proteins (see Taylor *et al.*[7a]).

To a very large extent then, following a sudden change in V_m the membrane current will be purely ionic after the capacity transient. This transient will depend on the electronics employed in the feedback system used to clamp the voltage (Section 10.3.4).

The excitability properties of nerve and muscle membranes result from the fact that the membrane ionic conductances are voltage dependent. These conductances result from the flow of ions (most often sodium, potassium, and calcium) through imperfectly selective membrane channels, and the magnitude of the conductance depends upon the fraction of channels that are open (for reviews, see Ehrenstein and Lecar[8] and Taylor.[8a] For the squid axon membrane, the behavior is well described by the empirical equations of Hodgkin and Huxley,[9] and an excellent introduction can be found in Katz.[10] The important point for our purposes is that the current-voltage relations contain a region of negative resistance such that the system is stable under potential control.

One of the first attempts to determine the characteristics of a system of this kind using potential control was that of Bartlett[11] for an iron wire in contact with acid.[12–14] Bartlett was led to do this at the suggestion of K. S. Cole,[15] who later introduced this concept in the study of the squid giant axon with the use of electronic feedback.[7]

In order to proceed experimentally, it is necessary to establish conditions where a patch of membrane can be isolated over which the current and voltage are uniform (averaged over some smaller area); and much of the article will be concerned with this question. Cole[15] and Marmont[16] introduced techniques for isolating small regions of the squid giant axon membrane with the use of an internal current supplying electrode, and external guard system

[7a] R. E. Taylor, J. M. Fernández, and F. Bezanilla, *in* "The Biophysical Approach to Excitable Systems" (W. J. Adelman and L. Goldman, eds.). Plenum, New York, 1982.

[8] G. Ehrenstein and H. Lecar, *Ann. Rev. Biophys. Bioeng.* **1**, 347 (1972).

[8a] R. E. Taylor, *Ann. Rev. Phys. Chem.* **25**, 387 (1974).

[9] A. L. Hodgkin and A. F. Huxley, *J. Physiol. (London)* **117**, 500 (1952).

[10] B. Katz, "Nerve, Muscle and Synapse." McGraw-Hill, New York, 1966.

[11] J. H. Bartlett, *Trans. Electrochem. Soc.* **87**, 521 (1945).

[12] R. S. Lillie, *Biol. Rev. Cambridge Philos. Soc.* **11**, 181 (1936).

[13] U. F. Franck and R. FitzHugh, *Z. Elektrochem.* **65**, 156 (1961).

[14] R. Suzuki, *IEEE Trans. Bio-med. Eng.* **14**, 114 (1967).

[15] K. S. Cole, *Arch. Sci. Physiol.* **3**, 253 (1949).

[16] G. Marmont, *J. Cell. Comp. Physiol.* **34**, 351 (1949).

and electronic feedback. This system was improved by Hodgkin *et al.*[17,18] by the addition of an internal voltage measuring electrode. They introduced the term "voltage clamp."

More recently, voltage clamp methods have been extended to other aspects of the membrane current. Some of the most notable recent extensions of the voltage clamp method are the measurements of channel noise, single-channel current jumps, and gating currents. Channel noise is the excess electrical noise created by the random opening and closing of the molecular ionic channels in the membrane. Under favorable circumstances the discrete current jumps caused by the opening and closing of single channels can be resolved.[18a] The gating currents are the displacement currents within the membrane which occur when charged groups of the channel macromolecule are rearranged during channel opening or closing.[18b]

In this paper we describe the principles of single-cell voltage clamping and discuss the basic theory and difficulties found in different preparations. We do not consider results of voltage clamp experiments. For reviews of voltage clamping in general, see Cole and Moore,[19] Moore and Cole,[20] Moore,[21] and Katz and Schwartz.[22] For reviews of results of voltage clamping, see Hodgkin,[2] Ehrenstein and Lecar,[8] Taylor,[8a] and Bezanilla and Vergara.[22a]

10.2. General Principles of Voltage Clamp

In an ideal system the current measured (without distortion) would be that which was flowing across a region of membrane, where the potential would instantaneously and accurately follow some time sequence (the command potential) determined by the experimenter.

The ideal system is never achieved in practice, but in many cases can be approximated quite closely. Some of the limitations of the real case can be illustrated by a simple example. Suppose we would like to voltage clamp a region of a cylindrical cell. In order to control the potential, it is necessary

[17] A. L. Hodgkin, A. F. Huxley, and B. Katz, *Arch. Sci. Physiol.* **3**, 129 (1949).

[18] A. L. Hodgkin, A. F. Huxley, and B. Katz, *J. Physiol. (London)* **116**, 424 (1952).

[18a] E. Neher and B. Sakmann, *Nature (London)* **260**, 779 (1976).

[18b] C. M. Armstrong and F. Bezanilla, *J. Gen. Physiol.* **63**, 533 (1974).

[19] K. S. Cole and J. W. Moore, *J. Gen. Physiol.* **44**, 123 (1960).

[20] J. W. Moore and K. S. Cole, *Phys. Tech. Biol. Res.* **6**, 263 (1963).

[21] J. W. Moore, *in* "Biophysics and Physiology of Excitable Membranes" (W. J. Adelman, ed.), p. 143. Van Nostrand-Reinhold, Princeton, New Jersey, 1971.

[22] G. Katz and T. L. Schwartz, *J. Membr. Biol.* **17**, 275 (1974).

[22a] F. Bezanilla and J. Vergara, *in* "Membrane Structure and Function" (E. E. Bittar, ed.), Vol. 2, p. 53. Wiley (Interscience), New York, 1980.

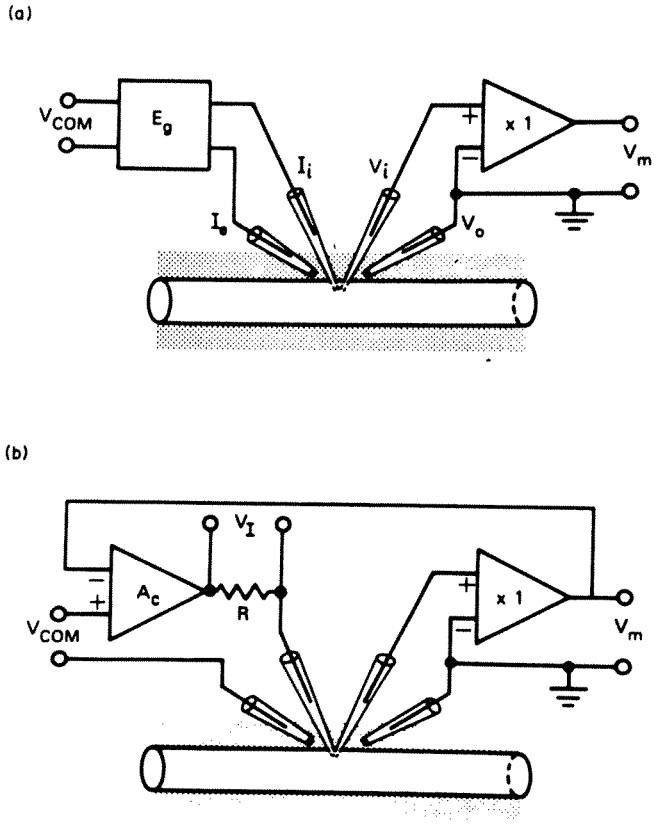

FIG. 1. Principle of controlling membrane voltage. (a) Schematic diagram of a system without feedback. (b) Schematic diagram of a voltage clamp system with negative feedback.

to measure it. We could introduce a microelectrode (Fig. 1a) and measure the membrane potential as the difference between the internal potential V_i and the external potential V_o, and supply current by another impaled microelectrode (I_i) and collect it with an external electrode (I_e). If the voltage generator (E_g) had zero output impedance and there were no resistance in the current path through the electrodes, we might be able to record a membrane voltage V_m identical to the command V_{COM}. These conditions are seldom possible to achieve.

We can improve this arrangement by use of negative feedback (Fig. 1b), where the measured voltage V_m is compared to the command V_{COM}, and the difference is amplified by an amplifier A_c that supplies the current necessary to make $V_m - V_{COM} = 0$. The current I_m required to control the voltage can be measured as the voltage drop V_I across a resistance R. Clearly $I_m = V_I/R$.

For a cylindrical portion of a cell the arrangement of Fig. 1b suffers from a serious defect. Although the potential at the point of the impaled voltage measuring microelectrode may be well controlled, the measured current comes not only from the immediate neighborhood of this electrode, but also

from other portions of the cell which may have nonuniform potential distributions. Under these conditions, the current is no longer being measured from a region of known and controlled potential. The errors could be more than just quantitative if the uncontrolled regions exhibit instabilities.[23] Spatial uniformity of current flow may be impossible to obtain for a membrane with nonuniform properties, but spatial uniformity of voltage can be approximated; when it is, it is referred to as a "*space clamp.*" Depending on the type and geometry of cells, the space clamp condition is obtained with a variety of methods. Axial wire is considered in Chapter 10.3; attempts with two and three microelectrodes in Chapter 10.4; patch isolation with pipettes in Chapter 10.5; and gap isolation is discussed in Chapter 10.6.

In the following discussion we assume perfect space clamp, and thus we picture the membrane subject to voltage clamp as a uniform patch of membrane. Later, we consider cases where the ideal is not met.

The basic circuit is pictured in Fig. 2. In this diagram we have represented one membrane patch as a box. The external electrode has a resistance of R_{eo} and the internal electrode a resistance R_{ei}. It is very common for the electrodes to be located at a certain distance from the surface of the membrane because there is connective tissue or adventitious cells surrounding the membrane under study. The electrical equivalent of these structures is a resistance in series with the membrane represented as R_s in Fig. 2. The resistance of the current electrode is represented by R_{ce}. A_c is an operational amplifier with open-loop gain A, and A_D is a differential amplifier with gain of 1. It is instructive to start with an idealized system where the input impedance of both amplifiers is infinite and the differential amplifier has a flat frequency response. Under these circumstances it is possible to derive the equation that relates V_M (the actual membrane voltage) to $-V_{COM}$ (the command voltage). The final result is

$$V_M = -\frac{-V_{COM} - I_m R_s - 2I_m(R_{ce} + R_s)/A}{1 + 2/A}. \tag{10.2.1}$$

This equation shows that the accuracy of the clamp not only depends on A but also includes membrane properties (unless R_{ce} and R_s are zero). In the ideal case, $A \to \infty$ for all frequencies, and

$$V_M = V_{COM} + I_m R_s. \tag{10.2.2}$$

Note that the actual membrane voltage is *never equal to the command voltage unless the membrane current or the series resistance is zero.* However, V_m,

[23] R. E. Taylor, J. W. Moore, and K. S. Cole, *Biophys. J.* **1**, 161 (1960).

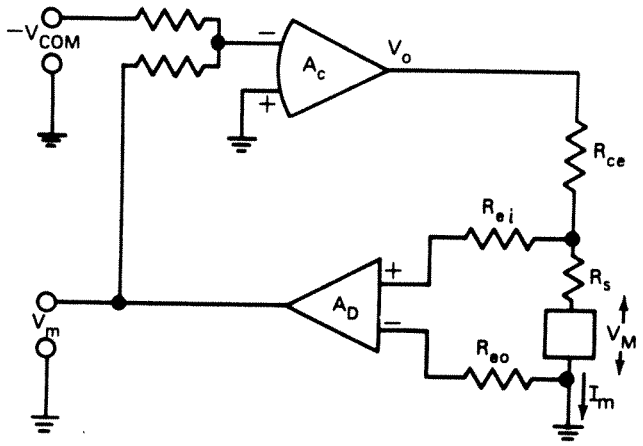

FIG. 2. Basic diagram of a voltage clamp system. The box represents a patch of membrane. V_M is the actual membrane potential, V_m is the measured membrane potential, I_m is the membrane current, and V_{COM} is the command voltage. R_{ei}, R_{eo} and R_{ce} are the resistances of external voltage, internal voltage, and current electrodes, respectively. R_s is the resistance in series with the membrane.

the measured voltage, will be equal to the command voltage because $V_m = V_M - I_m R_s$. The effect of series resistance can be serious in the determination of the current–voltage characteristics of a membrane because the voltage across the membrane is not controlled and becomes current dependent.[18] For this reason the voltage electrodes should be as close as possible to the membrane surface. However, in some cases the biological preparation contains a permanent barrier that effectively prevents positioning the electrodes right at the surface; in this case, some positive feedback can be introduced to compensate for the effect of series resistance as we shall see in the chapter on axial-wire voltage clamping (Section 10.3.5).

In modern operational amplifiers A is very large at dc and low frequencies, and Eq. (10.2.2) is a good approximation for that frequency range. However, at high frequencies A decreases, and Eq. (10.2.1) should be used. In practice this means that all fast changes in imposed V_{COM} will not be followed by the membrane as can be seen by inspection of Eq. (10.2.1) when A is decreased, and the clamp will perform far from ideal. In this situation the current-electrode resistance R_{ce} becomes very important.

Another very important source of error in practical voltage clamp originates in the capacitances of the voltage electrodes, which, in combination with their resistances, act as low-pass filters. This filtering effect is normally aggravated by the differential amplifier, which never has a flat frequency response as assumed in the example. Under these conditions, it is clear that the control amplifier will not receive the correct measurement of membrane

voltage, but it will be distorted at high frequencies; this, in turn, will have the effect of producing a distorted error signal at the input of the control amplifier, which will be unable to clamp the membrane voltage at the commanded value. In some extreme situations the phase lag introduced by the measuring-electrodes–amplifier–membrane combination may be enough to render the whole system unstable. Some stability characteristics of axial-wire voltage clamping are discussed in Section 10.3.5.3. Attempts to decrease the response time usually increase the tendency of the clamp to oscillate, as does series-resistance compensation. We consider below some detailed stability analyses designed to produce a clamp system with series-resistance compensation and fast rise time without overshoots or oscillations in the membrane potential.

The above example illustrates the main features of a basic voltage clamp system which we can now summarize:

1. Measurement of membrane potential should be made with low-impedance electrodes and positioned as close as possible to the membrane.
2. The current should be measured from a region where the voltage is controlled and uniform.
3. Current electrodes should be of low impedance.
4. Amplifiers should introduce minimum alterations and phase shift in the frequency range of interest.

10.3. Axial-Wire Voltage Clamp

In the case of long cylindrical cells, the space clamp condition can be approximated with the use of a long wire inserted axially as described in Section 10.3.1. This technique is restricted to cells of diameters large enough to allow penetration of the axial wire without damage to the membrane properties.

The large diameter of the giant axon of the squid makes it almost an ideal preparation to study the electrical properties of excitable membranes. In fact, the first voltage clamp system was built to control the membrane potential of squid axons.[15,16] Hodgkin *et al.*[17,18] and Hodgkin and Huxley[9] made their classic description of the ionic currents using a voltage clamp system in the squid giant axon. In the squid axon it is possible to introduce relatively large electrodes from one cut end of the fiber. A longitudinal low-resistance current electrode can also be introduced from the ends (axial wire) and serves the dual purpose of passing current and attaining space clamp conditions.

The axial-wire voltage clamp has been also used in other preparations such as *Myxicola* axons,[24] crayfish axons,[25] and barnacle muscle fibers.[26,27]

10.3.1. Cable Theory of an Axon with Axial Wire in Voltage Clamp

The axial wire is usually made of a solid platinum wire coated with platinum black. As a metal its resistance is very low, but when it is in contact with an electrolytic solution like the axoplasm, its surface impedance can be large, depending on frequency and the amount and direction of current passing through the metal–solution interface. The minimum representation of an axial wire inside an axon must include the surface resistance of the wire; an equivalent circuit[23] of a segment of length Δx is presented in Fig. 3a, where we have assumed zero external resistance to simplify treatment.† Note that points A and B are at the same potential V_a; therefore the representation of Fig. 3b is still equivalent which, in turn, can be represented in equivalent form by Fig. 3c. This is the familiar representation of a cable in which the membrane element (the box in the figure) is in parallel with a series combination of a voltage generator V_a (the axial-wire voltage) and a resistance r_a (the surface resistance per unit length of the axial wire).‡ Now we can find the value of the space constant of the combination axon and axial wire. For this purpose we represent the membrane by a Thevenin equivalent of a battery ε_m in series with the membrane resistance r_m as pictured in Fig. 4a. The final step is to obtain the equivalent of Fig. 4a as pictured in Fig. 4b, where

$$r = r_m r_a/(r_m + r_a), \qquad \varepsilon = (V_a r_m + \varepsilon_m r_a)/(r_a + r_m);$$

r is the parallel combination of the membrane resistance and the wire surface resistance. A good axial wire will have r_a much smaller than r_m; therefore r will be practically equal to r_a; furthermore, from the above

[24] L. Binstock and L. Goldman, *J. Gen. Physiol.* **54**, 730 (1969).
[25] P. Shrager, *J. Gen. Physiol.* **64**, 666 (1974).
[26] S. Hagiwara, H. Hayashi, and K. Takahashi, *J. Physiol. (London)* **205**, 115 (1969).
[27] R. D. Keynes, E. Rojas, R. E. Taylor, and J. Vergara, *J. Physiol. (London)* **229**, 409 (1973).

† The case of finite external resistance is given in Taylor *et al.*[23]

‡ In a more general treatment the surface impedance per unit length of the axial wire, z_a, replaces r_a; it is defined as the Laplace transform of the voltage divided by the Laplace transform of the current per unit length of wire. The same equations can be used by simply replacing r_a by z_a and the time solution can be obtained by the use of tables or the complex inversion formula.

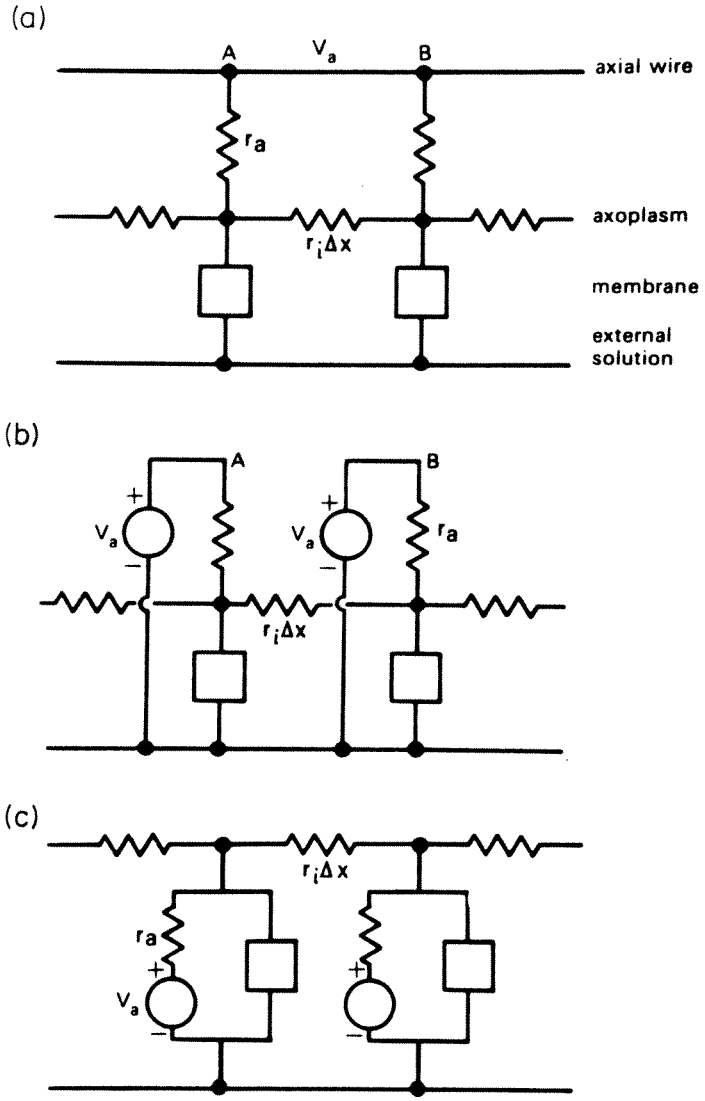

FIG. 3. Schematic diagram of an axon segment with axial wire: (a) simplified representation before reduction; (b) and (c) equivalent circuit after circuit reduction. For details see text.

equation it can be seen that ε will be very close to V_a. The space constant of the axon–axial wire combination will be

$$\lambda = \sqrt{r/r_i}. \tag{10.3.1}$$

The above equations show that as the axial wire is made of lower surface resistance, λ decreases. This is in direct contradiction with the general idea that the introduction of an axial wire in an axon makes its space constant larger. It is clear, however, from the derivation presented that the effect of the axial wire is exactly the opposite; it shortens the space constant, making each patch of membrane more independent of its neighbors but at the same time imposing a voltage V_a in each patch. This effect is desirable to isolate

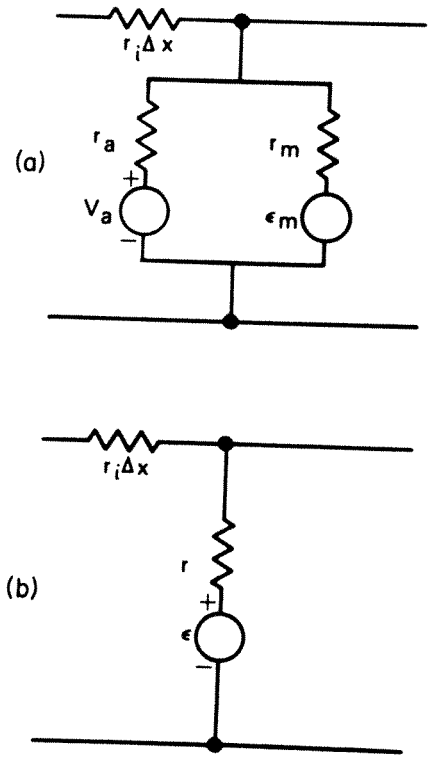

FIG. 4. Thevenin equivalent of a segment of an axon of length Δx containing an axial wire connected to a voltage source at potential V_a. (a) Equivalent circuit of a patch with axial wire. (b) Thevenin equivalent of a membrane patch with axial wire.

patches of membrane that do not have exactly the same properties as the rest of the membrane; in particular, it isolates end effects. This can best be illustrated solving the cable equation for a terminated cable using the circuit elements indicated in Fig. 4b.

The equation to be solved is

$$d^2V/dx^2 = (V - \varepsilon)/\lambda^2, \tag{10.3.2}$$

where steady state and a constant value for r are assumed.† Normally, the axon is penetrated in both ends with electrodes and perfusion cannula. We can approximate the boundary conditions by the expression

$$V(x) = -\frac{1}{r_i}\frac{\partial V}{\partial x} R_g \quad \text{at} \quad x = 0 \quad \text{and} \quad x = l, \tag{10.3.3}$$

where R_g is the short-circuit resistance at the ends and r_i is the internal resistance per unit length.

---

†Note that when the membrane resistance is negative, λ will be imaginary. However, the equations still hold and the solutions will contain trigonometric sines and cosines. For a discussion of this case see Cole[7] (p. 342).

The solution of the differential equation (10.3.2) with the above boundary condition (10.3.3) is

$$V = \varepsilon\left(1 - \frac{\sinh(x/\lambda)}{[1 + R_g/r_i\lambda]\sinh(l/\lambda)}\right.$$

$$\left. - \frac{\sinh[(l-x)/\lambda] + (R_g/r_i\lambda)\cosh[(l-x)/\lambda]}{[1 - (R_g/r_i\lambda)^2]\sinh(l/\lambda)}\right). \quad (10.3.4)$$

To simplify the situation, let us assume further that $R_g = 0$, which is equivalent to a short circuit at both ends. The membrane potential distribution is given by

$$V = \varepsilon\left(1 - \frac{\sinh(x/\lambda) + \sinh[(l-x)/\lambda]}{\sinh(l/\lambda)}\right). \quad (10.3.5)$$

As the membrane is voltage clamped, the membrane potential in the center of the fiber is equal to the command voltage V_{COM}

$$V_{COM} = V(l/2);$$

then

$$\varepsilon = V_{COM}\Big/\left(1 - \frac{2\sinh(l/2\lambda)}{\sinh(l/\lambda)}\right),$$

and the voltage distribution in the voltage clamp will be

$$V(x) = V_{COM}\left(\frac{\sinh(l/\lambda) - \sinh(x/\lambda) - \sinh[(l-x)/\lambda]}{\sinh(l/\lambda) - 2\sinh(l/2\lambda)}\right). \quad (10.3.6)$$

Figure 5 shows the distribution of V/V_{COM} along the axon for different values of the space constant. It is clear that the smaller the space constant the more homogeneous is the potential along the axon, because end effects are circumscribed to smaller regions. Therefore the best space clamp is achieved when the surface resistance of the axial wire r_a is lowest. Very low-resistance axial wires can be prepared by platinizing the platinum wire,[20] but their resistance becomes very high when steady current is passed. This latter situation appears frequently when an axon is held at a potential different from its resting potential; under these conditions the space clamp may be far from ideal.

10.3.2. Giant Axon Preparation

As explained above, the axial-wire technique can only be used on large cells, and it has been successful with squid giant axon, crayfish axon, *Myxicola* axon, and barnacle muscle fibers. The experimental procedures are

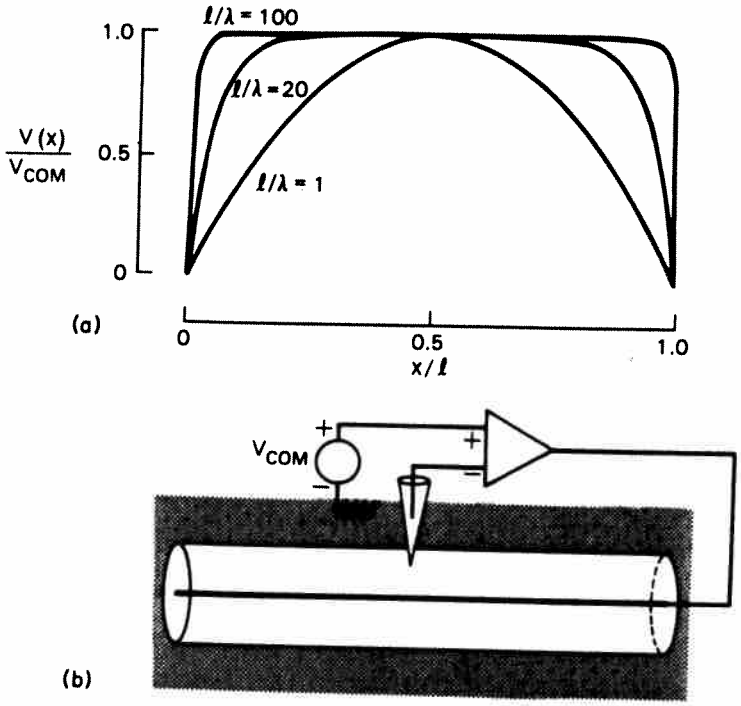

FIG. 5. Potential distribution inside an axon containing an axial wire. (a) The normalized steady-state potential distribution as calculated from Eq. (10.3.6) for three different values of l/λ, where l is the length of the fiber and λ is the space constant. The axon is voltage clamped, as indicated in (b), and the potential is controlled in the center.

similar for all these preparations. To familiarize the reader with this technique, we shall briefly describe the squid giant axon preparation.

10.3.2.1. Isolation of the Giant Axon. The giant axon from the stellate ganglion has been obtained from several species of squid: *Loligo forbesi*, *Loligo pealei*, *Loligo vulgaris*, *Loligo opalescens*, *Dosidicus gigas*, *Doritheutus plei*, and others. The axon diameter varies among different species and ranges between 200 nm and 1.3 mm. Normally, axons are dissected out of the squid mantle in running seawater, and they are later cleaned of other fibers and connective tissue under microscope dissection. For a more detailed description see, for example, Gilbert.[28] Cleaned segments from 2 to 8 cm long are tied at the ends with threads and can be kept for several hours at 4–8°C in seawater.

10.3.2.2. Experimental Chamber and Internal Perfusion. The details of the experimental chamber differ depending on whether the axon is held horizontally or vertically. Several designs have been used successfully.[18,20,29,30]

[28] D. L. Gilbert, *in* "A Guide to Laboratory Use of the Squid, *Loligo pealei*." Mar. Biol. Lab., Woods Hole, Massachusetts, 1974.

[29] W. K. Chandler and H. Meves, *J. Physiol.* (*London*) **180**, 788 (1965).

[30] C. M. Armstrong, F. Bezanilla, and E. Rojas, *J. Gen. Physiol.* **62**, 375 (1973).

The method used to internally perfuse the axon has also influenced the design of the chamber. Two general types of perfusion methods have been described: the roller technique originally described by Baker *et al.*,[31] in which the axoplasm is extruded by a roller and the axon later reinflated by the perfusion solution; the cannulation technique originally described by Oikawa *et al.*,[32] in which the axoplasm is sucked into a cannula as the cannula is advanced along the axon.

In the following, we briefly describe the Tasaki technique,[32] as modified by Fishman,[33] to illustrate one of the methods to perfuse and voltage clamp a squid axon. The axon segment is positioned in the chamber as illustrated in Fig. 6, which is based on the chamber designed by Armstrong.[30] A cut is made with a microscissors at point A, and a glass cannula (PC) is inserted into the axon and advanced with the aid of a micromanipulator. As the cannula is advanced, microscope observation is required to maintain the cannula centered in the axis of the axon. Normally, a small prism is used to visualize the position of the cannula in the vertical plane. Simultaneously with the advancing of the cannula, mouth suction is applied, and the axoplasm is sucked into the cannula lumen. At point B another cut is made, and the cannula is pushed outside the axon. The axoplasm inside the cannula is blown away, and the flow of the internal perfusion solution is started through the cannula. The composite electrode described in Section 10.3.2.3 is introduced partially inside the cannula, and then the cannula is pulled back as the electrode is pushed in. Normally, the air gap (region between B and C) is treated with a protease, such as papain or pronase, for about one and a half minutes by positioning the tip of the cannula at C and letting the internal perfusion solution containing the enzyme flow freely. Finally, the cannula is retrieved almost to point A as the electrode is pushed to the final position that requires the tip of the voltage pipette to be in the center of the chamber.

10.3.2.3. Internal Electrodes. Several types of internal electrodes have been used for voltage clamping. The classical combination electrode described by Hodgkin *et al.*[18] consists of two silver-chlorided silver wires twisted into a double spiral on the glass rod. One of the wires was used to measure potential (voltage electrode) and the other was used to pass current (axial wire). The main disadvantage of this electrode is that inside the unperfused axon it does not measure steady dc potential because the voltage electrode is not stable. One of the most commonly used combination

[31] P. F. Baker, A. L. Hodgkin, and T. I. Shaw, *J. Physiol.* (*London*) **164**, 330 (1962).

[32] T. Oikawa, C. S. Sypropoulos, I. Tasaki, and T. Teorell, *Acta Physiol. Scand.* **52**, 195 (1961).

[33] H. M. Fishman, *Biophys. J.* **10**, 799 (1970).

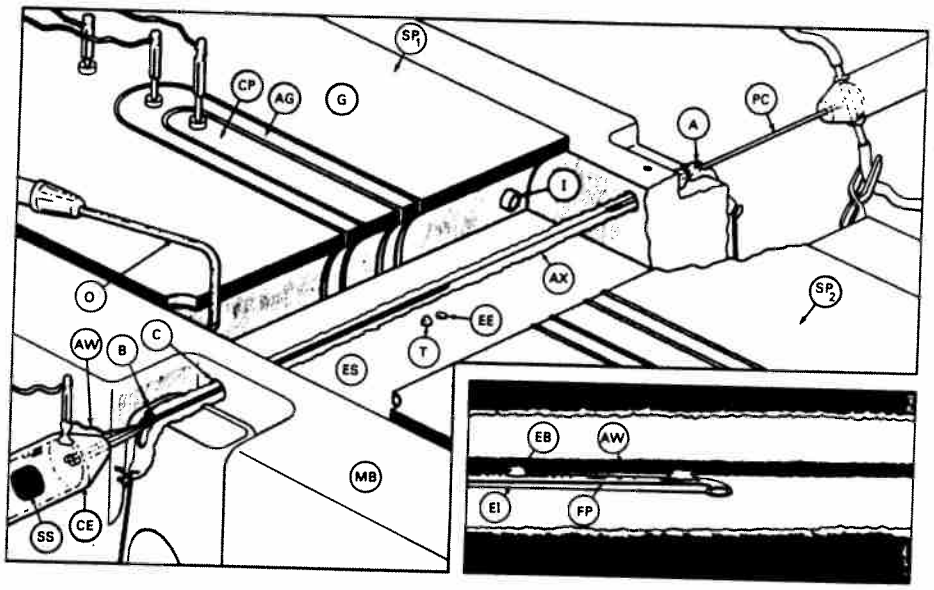

FIG. 6. Squid axon chamber. The main body of the chamber (MB) is made of Lucite. The two silver plates SP_1 and SP_2 are movable and can be approached to enclose the axon (AX). SP_1 is thermally connected to a Peltier cooler that is connected to a feedback loop to control the chamber temperature measured by thermistor T. The external solution (ES) is precooled by passing it inside the silver block before it enters the chamber through inlet I. The solution is sucked away by outlet O. The plates are made of several sections (*G*, guard; AG, auxiliary guard; CP, central or measuring plate) separated among them by thin sheets of Mylar. The faces of the plates in contact with the external solution are platinized (darker regions). The perfusion cannula (PC) enters in the axon at point A and the combination electrode (CE) at point B. Inside the combination electrode the silver–silver chloride pellet (SS) can be observed. The tip of the external electrode is at the bottom in the center of the chamber (EE). (The length of the perfusion cannula PC has been drawn shorter to fit the diagram. Its real length should span at least from point A to B, which is about 20 mm.) Inset: detail of the internal combination electrode inside the axon. AW is the axial wire, EI is the cannula of the potential-measuring electrode, and FP is a floating platinum wire. The glass cannula EI is glued to the platinized axial wire AW with small epoxy beads (EB).

electrodes is that described by Chandler and Meves,[29] which consists of a platinized platinum wire (axial wire) used to pass current and a cannula attached to it to measure the potential. The cannula is normally filled with 0.6 *M* KCl and acts as a salt bridge between the axon interior and a reversible hemicell of Ag–AgCl or calomel. To decrease the high-frequency impedance of the cannula, a floating platinum wire is positioned inside (Fig. 6). Sometimes the floating Pt wire is platinized.[34]

10.3.2.4. External Electrodes. The external voltage electrode is simply a salt bridge with one end positioned as close as possible to the axon and the other end in contact with a Ag–AgCl or calomel hemicell.

[34] H. M. Fishman, *IEEE Trans. Biomed. Eng.* **BME-20**, 380 (1973).

The external current electrode has been made in several different ways. The most common approach is to position two platinized surfaces made of silver or platinum on either side of the axon. Each surface is divided into three electrically isolated plates: a central electrode or measuring electrode and two lateral electrodes also called guards. These large metal electrodes both pass current and, at the same time, contribute to the space clamping. Normally, the guard electrodes are grounded and the central electrode is held at virtual ground and current is measured only with that electrode. See Fig. 6 for an example of a central plate and several guards used to verify homogeneity along the axon.

10.3.3. Measurement of Membrane Current

As mentioned earlier, one would like to collect all of the current flowing through a region of membrane over which the voltage is uniform; several different methods have evolved for doing this. We shall discuss the use of lateral guards, external differential electrodes, external pipettes, and gap isolation techniques (Chapter 10.6).

When an axial wire is used to supply current, the effects of voltage nonuniformities near the ends can be reduced with the use of lateral guards. In this method three external electrodes are employed and the current measured only from the central one, either by passing it through an external resistance and measuring the potential across it,[16,17] or by means of a current-to-voltage converter.[19] Various modifications of the precise form of the external electrodes have been used,[19,35] and the type in most common use today[36,37] consists of three pairs of electrodes forming the sides of a rectangular trough. In some systems the three chambers are separated by partitions, and some Vaseline/oil mixture is used for insulation. Except for considerations of noise (Section 10.3.4), it is not clear that this is an improvement over using no partitions. If the axon is uniform and the guards are long enough, the partitions are not needed; unless the insulation is quite perfect, any current flowing through the gap could produce voltage drops across the membrane which might aggravate the spatial nonuniformities. A system with thin plastic partitions used to record ionic and gating currents has been recently reported.[46]

Regardless of the arrangement for measuring current, there is the important experimental question of how one knows that the current distribution is indeed uniform. This has been investigated with the use of two small closely spaced external differential electrodes for measuring current density over

[35] I. Tasaki and S. Hagiwara, *J. Gen. Physiol.* **40**, 859 (1957).

[36] E. Rojas and G. Ehrenstein, *J. Cell. Comp. Physiol.* **66**, Suppl. 2, 71 (1965).

[37] E. Rojas, R. E. Taylor, I. Atwater, and F. Bezanilla, *J. Gen. Physiol.* **54**, 532 (1969).

small regions of the squid giant axon.[19,20,23,37] At first this would seem an ideal way to measure current, but there are problems of sensitivity, noise, and calibration. It is still true, however, that we know of no other way to check membrane current uniformity except with the use of multiple external longitudinal electrodes (Section 10.3.2.4 and Fig. 6). Narrow C-shaped external electrodes have been used for current measurement[29] and for checking uniformity in the case of radioactive tracer measurements where the use of guards was not possible.[37a]

We do not know of a theoretical analysis for the precise geometry employed with external differential electrodes. Chandler and Meves[29] present an approximate solution in connection with their method of calibration using the simplifying assumption that the two external electrodes see the current arising from a point within the axon, as if they were on two equipotential concentric spheres. We have derived that an electrode in a medium of resistivity R_e (Ω cm) at a radial distance r from the center of a cylinder of radius a and longitudinal position z has a potential due to a thin ring of current at $z = 0$ of

$$V(r, z) = \frac{i_0 R_e}{\pi} \int_0^\infty \frac{K_0(\omega r)}{\omega K_1(\omega a)} \cos(\omega z)\, d\omega, \tag{10.3.7}$$

where K_0 and K_1 are modified Bessel functions. Numerical computations of Eq. (10.3.7) give results that are different from those obtained with the simplified model of Chandler and Meves.[29]

Davies[38] and Jaffe and Nuccitelli[39] have used a single vibrating electrode in place of the differential pair. It would seem from the analyses that have been done that the potential of a single external electrode close to the membrane would be a good approximation to the underlying membrane current.

Another way to measure membrane current is to apply an external pipette to the surface. If the internal resistance of the pipette is small compared to the leak around the tip, the method is successful (Chapter 10.5). One must either use a cell whose membrane is not covered by "extraneous coats" (i.e., single muscle fibers treated with collagenase or tissue-cultured cells) or bathe the region around the tip with sucrose solutions which can penetrate the connective tissue or Schwann cell layer. The use of suction can be helpful (Chapter 10.5). If the tip is small enough, it is possible to observe single channels.[18a] This is extremely important in that it not only allows direct determination of the conductance of single channels but also provides a powerful tool for studying channel mechanisms.

[37a] I. Atwater, F. Bezanilla, and E. Rojas, *J. Physiol. (London)* **201**, 657 (1969).
[38] P. W. Davies, *Fed. Proc., Fed. Am. Soc. Exp. Biol.* **25**, 332 (1966).
[39] L. F. Jaffe and R. Nuccitelli, *J. Cell Biol.* **63**, 614 (1974).

The last, and very little tried, method is the use of a pipette (Westerfield,[40] Llano and Bezanilla[41]) or metal electrode (Taylor and Bezanilla[41a]) which is connected to a current-to-voltage converter and draws off some of the current on its way to the main external electrode. The so-called gap isolation techniques are probably the most widely used methods of measuring current at this time and are extensively discussed in Chapter 10.6.

10.3.4. Electronics for the Voltage Clamp System

Many voltage clamp diagrams used for squid axons have been published. The system used by Hodgkin *et al.*[18] has a very short settling time, but it cannot control the membrane potential for long periods of time because the voltage electrode does not measure steady-state potentials (see Section 10.3.2.3). However, the system is perfectly appropriate to impose changes of potential across the axonal membrane. The major changes introduced by Moore and Cole[20] were to incorporate a microelectrode to measure the true membrane potential and the use of operational amplifiers. Since then, operational-amplifier performance has improved noticeably, and very fast clamps can now be built with commercially available units using the combination electrode described in Section 10.3.2.3.

Figure 7 is a schematic diagram of one possible voltage clamp system that has been used successfully in our laboratory. The membrane potential is measured by the differential combination A_1, A_2, and A_3. Special care must be exercised to minimize capacitative loading at the input to prevent filtering of high-frequency components. The membrane voltage is summed to the negative of the steady membrane potential desired (the holding potential HP) plus the pulses or waveforms to be imposed on the axon (the imposed waveform V_p) at the summing junction of operational amplifier A_4. The combination C_V and R_V act as a lead compensator and C_L and R_L as a stabilizing network. We have also (at the suggestion of R. Levis) found that the use of a lead compensator in the current feedback for series-resistance compensation (Section 10.3.5) provided by C_I is helpful. The output of the operational amplifier A_4 is connected directly to the axial wire when the voltage clamp is on or connected to an auxiliary feedback when the clamp is off. The voltage clamp can be turned on remotely by replacing the switch S_1 by two field-effect transistors connected as switches or using two bipolar transistors.[42] This electronic switch makes it possible to interrupt the free course of the action potential to study the ionic conductances during the

[40] M. Westerfield, personal communication.

[41] I. Llano and F. Bezanilla, *Proc. Natl. Acad. Sci. U.S.A.* **77**, 12 (1980).

[41a] R. E. Taylor and F. Bezanilla, unpublished observations.

[42] F. Bezanilla, E. Rojas, and R. E. Taylor, *J. Physiol. (London)* **211**, 729 (1970).

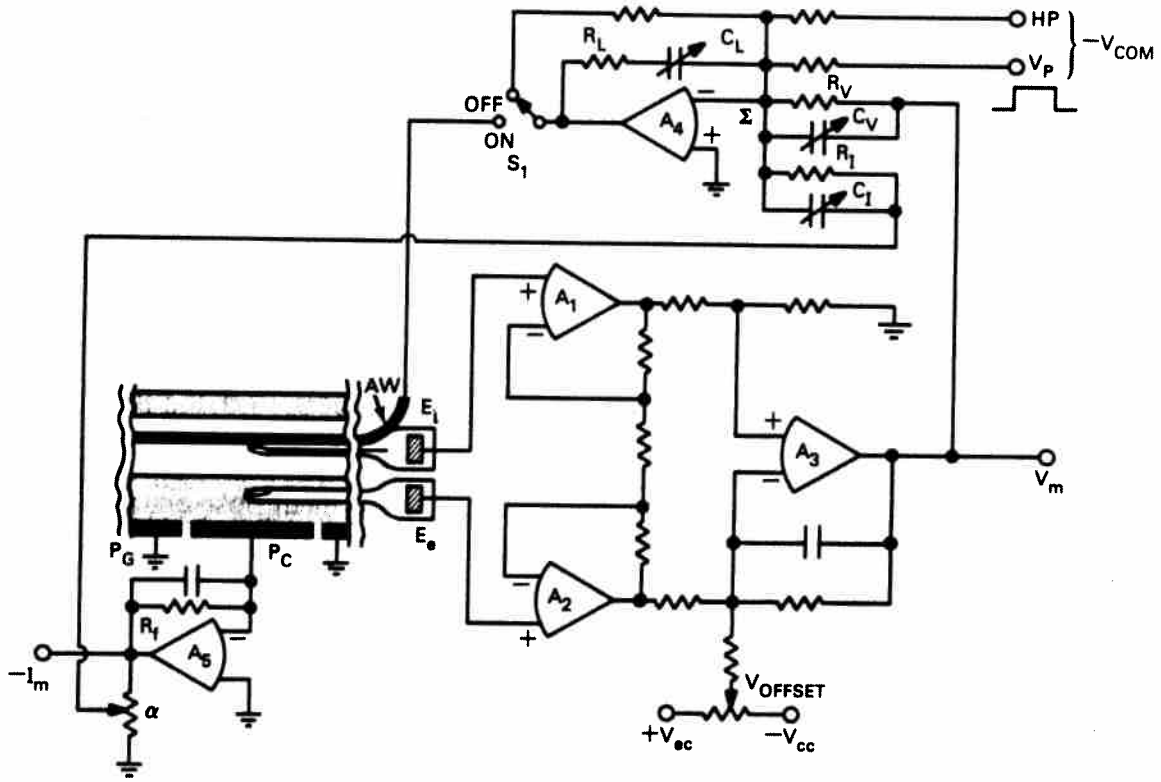

FIG. 7. Schematic diagram of a squid-axon voltage clamp. A_1 and A_2 are very high-input-impedance, low-input-capacitance, wide-bandwidth operational amplifiers wired in a voltage follower configuration to measure the potential of the internal electrode E_i and external electrode E_e. A_3 is an operational amplifier connected as a differential amplifier giving the difference between the outputs of A_1 and A_2 as V_m, the membrane voltage. V_{OFFSET} is used to compensate for electrode and junction potentials. Amplifier A_4 is the control amplifier, and its summing junction $\sum$ sums the negative of the desired potential (V_{COM}), which consists of a steady potential (HP) and a waveform (V_P) such as a pulse pattern, the membrane voltage (V_m), and a fraction of the negative of membrane current ($-\alpha I_m$) for series resistance compensation. Note that V_m is connected to $\sum$ through R_V in parallel, with C_V acting as a lead compensator. C_L and R_L are a stabilizing network. S_1 is a switch that connects the output to either the axial wire (AW): clamp in position ON, or to an auxiliary feedback loop: clamp in position OFF. Membrane current derived by the central plate (P_C) is connected to the negative input of operational amplifier A_5, whose output will be equal to the negative of the current derived by P_C times the feedback resistor R_f. The high gain of A_5 guarantees that P_C is held at the same ground potential as the guard plates P_G, which are connected directly to ground; however, at high frequencies the gain decreases and P_C may not be at ground potential Examples of commercially available amplifiers A_1 and A_2 are National Semiconductors LF356; of A_3, A_4 and A_5 are National Semiconductors LF357.

spike. Also, it can be used to protect the axon from electrical transients that could drive the membrane potential beyond safe limits. This is accomplished by measuring the membrane potential at all times and activating a bistable flip-flop whenever the membrane potential reaches unsafe limits. The output of the flip-flop is used to control the electronic switch to open the clamp loop.

The current amplifier A_5 is connected as a current-to-voltage converter with the input connected directly to the measuring plate (central). This makes the central plate potential equal to ground potential when the amplifier has a very large gain. However, it must be remembered that the open-loop gain of operational amplifiers decreases with frequency, and therefore at high frequencies the central plate will not be at ground potential, making a gradient of potential in the external solution along the axon (see Section 10.4.1). It is important then to select an amplifier with a large gain–bandwidth product to maintain space clamp over the entire frequency range of interest during voltage clamping.

Unless partitions are used, the resistance between the central plates and the guards is quite low because it is given by the external solution. This low-resistance pathway between the summing junction and ground drains a large current from the input voltage noise generator of the operational amplifier, producing significant noise at the output of the current amplifier. Frequently, this is the predominant source of noise in the voltage clamp system, and it can be minimized using current amplifiers with low input voltage noise.

Levis[43] has analyzed the noise performance for a clamp and concluded that the major source of noise is the voltage measuring electrodes if the resistance between the center chamber and the guard chambers is high. If this resistance is low (10 Ω, say), this may become the major source of noise. This problem may be avoided by not using guards[44,45] or by the use of insulating partitions.[46]

10.3.5. Series-Resistance Compensation

As mentioned above, the electrodes should sense the potential as close as possible to the membrane. In the squid axon, the Schwann cell layer constitutes a barrier that cannot be penetrated by the electrodes, and a significant resistance is included in series with the axolemma. The origins of this resistance are the narrow clefts between Schwann cells, which amounts to about 4 Ω cm^2,[18,47,56] but it varies considerably with the type of external solution and possibly with the state of the axon.

Hodgkin *et al.*[18] introduced in their clamp circuitry positive feedback that subtracted the voltage drop across the series resistance (compensated

[43] R. Levis, Doctoral Dissertation Department of Physiology, University of California, Los Angeles, 1981.

[44] E. Wanke, L. J. DeFelice, and F. Conti, *Pfluegers Arch.* **347**, 63 (1974).

[45] F. Conti, L. J. DeFelice, and E. Wanke, *J. Physiol (London)* **248**, 45 (1975).

[46] F. Bezanilla, R. E. Taylor, and J. M. Fernández, *J. Gen. Physiol.* **79**, 21 (1982).

[47] L. Binstock, W. J. Adelman, Jr., P. Senft, and H. Lecar, *J. Membr. Biol.* **21**, 25 (1975).

feedback). In Fig. 7 a similar arrangement has been incorporated. A voltage proportional to a fraction of the membrane current equal to $-\alpha I_m R_f$ is added to the measured V_m at the summing junction of amplifier A_4. If α is adjusted to make this voltage equal to the $I_m R_s$ voltage, the control amplifier A_4 will impose the command voltage plus holding potential on $V_m - I_m R_s$, which is the real membrane potential V_M [see Fig. 2 and Eq. (10.2.2)].

10.3.5.1. Effects of Series Resistance. If the electronics yielded a perfect clamp, i.e., the measured potential faithfully followed the command potential, there would still be errors introduced by uncompensated series resistance. These errors have been discussed by many people including Hodgkin *et al.*[18] (pp. 430, 435), Taylor *et al.*,[23] and Binstock *et al.*[47] We may distinguish three cases: (i) passive membranes which may be described by models containing elements which do not vary with voltage, current, or time; (ii) active membranes where the region of interest contains only current–voltage curves at any given time (isochronal curves), which are straight lines with positive slope; and (iii) systems in which the isochronal current–voltage curves in some region are either curved and varying with time or there is a transient or steady-state negative resistance region. In the first two cases, the data as recorded could be corrected with the use of a load line for a known series resistance. In case (iii), it may not be possible to make corrections. Not much can be added to the discussion of these points in Taylor *et al.*,[23] and the computer plots of current versus time for solutions of the equations of Hodgkin and Huxley in Binstock *et al.*[47] For more detailed studies of stability in the negative-resistance region as affected by series resistance, and the stability of the second patch in the model of Taylor, see Chandler *et al.*[48]

We may summarize here by saying that in studies of the squid giant axon in voltage clamp, the addition of series resistance produces changes in the shape of the current–time curve in response to an applied voltage step and changes in the peak inward and steady-state outward current–voltage curves. Load-line corrections, as predicted, correct for the linear portions of the peak inward and steady-state outward curves, but not for the maximum peak inward current or the shape of the peak inward current curves in the negative-resistance region. The time to peak of the transient inward current was corrected by the use of a load line over most of the curve. Taylor *et al.*[23] also demonstrated that, for their system, addition of negative-resistance compensation did correct, to a large degree, for the effects of removing the external reference electrode, which was, in fact, an addition of series resistance.

[48] W. K. Chandler, F. FitzHugh, and K. S. Cole, *Biophys. J.* **2**, 105 (1962).

It is then advisable to perform experiments using series-resistance compensation in order to measure the real current–voltage characteristics of the membrane. The first step to compensate for series resistance is an accurate determination of its value; we address this problem in the next section

10.3.5.2. Determination of Series Resistance. The measurement of the resistance in series with the membrane and between the voltage measuring electrodes would be a fairly simple matter if (i) the membrane capacitances were loss free, (ii) the series elements were pure resistance, and (iii) the applied pulses and measurements were not distorted by electrode impedances and amplifier delays. In this case, the most accurate way would probably be to measure the impedance and extrapolate to infinite frequency. The most rapid would be to apply a rectangular pulse of current and extrapolate the measured voltage to zero time. It would also be possible to apply a voltage clamp pulse and fit the measured current. All of these methods have been used, with variable and confusing results.

10.3.5.2.1. Lossy Capacitance. Curtis and Cole,[6] using transverse currents with external electrodes, measured the impedance of the axon membrane and concluded that the capacitance was lossy and could be approximated over their frequency range by a constant-phase-angle impedance of the form $Z_{cc} = Z^* (j\omega\tau)^{-\alpha}$, where $j = \sqrt{-1}$, $\omega = 2\pi f$, and f is the frequency. They reported an average α of 0.85, representing a constant phase angle of $\phi = \alpha\,(90°) = 76°$. Using internal and external electrodes, Hodgkin *et al.*[18] concluded that their capacity transient for a voltage clamp pulse was roughly consistent with a phase angle of 80° (but see FitzHugh and Cole[49]). Taylor and Chandler,[50] using internal and external electrodes with a bridge, found that between 10 and 70 kHz the impedance closely fit the constant-phase-angle expression above, with comparable values for α.[51] Taylor[52] later showed that the same data could be fairly well approximated by a single relaxation-time Debye-type dielectric (and fit very well for a moderate distribution of relaxation times). FitzHugh and Cole[49] have computed voltage and current transients for the constant-phase-angle capacitance with parallel leakage conductance and series resistance. Their results could be compared with experimental results if such were available. A treatment of the transient response to an applied current of the form $I(t) = I_0(1 - e^{-t/\tau})$ can be found in Binstock *et al.*[47] for a capacitative element with a single-relaxation Debye-type dielectric with parallel leakage and series resistance.

[49] R. FitzHugh and K. S. Cole, *Biophys. J.* **13**, 1125 (1973).
[50] R. E. Taylor and W. K. Chandler, *Biophys. Soc.* (*Abstr.*) TD1 (1962).
[51] N. Matsumoto, I. Inoue, and U. Kishimoto, *Jpn. J. Physiol.* **20**, 516 (1970).
[52] R. E. Taylor, *J. Cell. Comp. Physiol.* **66**, 21 (1965).

10.3.5.2.2. SERIES IMPEDANCE. The squid giant axon is surrounded by a Schwann cell layer which would not have a pure-resistance impedance. This is probably not serious in most cases because it approximates a pure resistance for frequencies below 100 kHz.[53]

10.3.5.2.3. FINITE RESPONSE TIME. Hodgkin *et al.*[18] reported the results of two experiments in which they determined the membrane capacitance and series resistance for the squid giant axon membrane using rectangular pulses of current. They considered that the amplifiers for measuring current and voltage had equal response times and that the effect would cancel. This is an important concept so we shall elaborate somewhat. Consider Fig. 7. The membrane potential is given by $V_M = I_m R_s + (1/C_m)_0 \int_0^t I_m\, dt'$. Denoting the Laplace transform with argument s by an overbar, for $I_m(0) = 0$ we find

$$\bar{V}_M(s) = \bar{I}_m(s)R_s + (1/C_m)\bar{I}_m(s)/s.$$

Say the electrodes plus amplifiers distort the measurement of V_M and I_m into V'_M and I'_m, where the transfer functions are given by $Y_v(s) = \bar{V}'_m(s)/\bar{V}_M(s)$ and $Y_i(s) = \bar{I}'_m(s)/\bar{I}_m(s)$. If $Y_v(s) = Y_i(s)$, they will indeed cancel, and we may use the equation we started with, but using the measured $V'_M(t)$ and $I'_m(t)$. In principle, for any applied current we may fit the measured curves and obtain values for C_m and R_s.

One way to reduce the effects of amplifier delays would be to slow down the time course of the applied current. Using a known finite-rise-time current pulse, Binstock *et al.*[47] derived the time course of the voltage for a capacity with parallel conductance and series resistance and presented results of measurements on squid axons and *Myxicola* central nerve cords. If the leak conductance is small, extrapolation of the linear portion of the voltage curve to zero time gives an intercept equal to $I_0 R_s = I_0 \tau/C_m$, where τ is the time constant of the rising phase of the current pulse.

A somewhat more elegant, but to our knowledge untried, scheme is presented by Cole and Lecar.[54] One may apply almost any shaped current pulse asymptotic to a constant and extract the series resistance in the following way: draw a straight line asymptotic to the late linear portion of the voltage record, pick a time t_0, integrate the difference between the straight line and the recorded voltage from $t = 0$ to $t = t_0$, and subtract this from the integral of the difference from $t = t_0$ to $t = \infty$; vary t_0 until the result is zero. The value of the voltage given by the straight line at $t = t_0$ is then equal to $I_0 R_s$, where I_0 is the value for a rectangular pulse giving the same voltage at long times.

[53] K. S. Cole, *Biophys. J.* **16**, 84 (1976).

[54] K. S. Cole and H. Lecar, *J. Membr. Biol.* **25**, 209 (1975).

For any of these approaches it is necessary to carefully consider the distortions produced by electrode impedances and amplifier delays for each particular case.

A very novel approach has been tried[55,56] in which voltage-sensitive dyes are employed. Application of a voltage clamp pulse which is rectangular as measured electrically results in a light response which, in the presence of a series resistance, will reflect the time course of the membrane current due to the $I_m R_s$ drop. For a nerve membrane where the sodium current component is large, the amount of negative-resistance compensation needed to make the response of the dye rectangular gives an estimate for the series resistance.

10.3.5.3. Voltage Clamp Stability and Series-Resistance Compensation. A thorough analysis of the properties of a voltage clamp system as actually employed would be very complicated, and most voltage clamp systems in use today are constructed on the basis of intuition and cut and try.

Katz and Schwartz[22] have considered a very simplified circuit in which the resistance (R_s in Fig. 2) in series with the membrane and between the voltage measuring electrodes is ignored and only the time constants of the membrane and the control amplifier are considered. This gives a second-order system which is probably insufficient to say very much about an actual system. They analyze the effect of a feedback arrangement to reduce the effects of the access resistance R_{ce} between the output of the current-supplying amplifier and the preparation. This is important when using microelectrodes (Chapter 10.4) to supply current, and in some of the cases that they consider the series resistance R_s is small. For squid axon membrane clamping the access resistance is small, and R_s is a major problem.

Levis[43,57] has done many voltage clamp analyses and has concluded that an important consideration for stability and a fast clamp, using negative-resistance compensation (for R_s), is that the frequency response characteristics of the voltage and current measuring systems be comparable and combined before feeding back to the control amplifier through a compensating network.

Consider Fig. 2 with the additional feature that the current is measured as shown in Fig. 7 and a voltage $-\alpha I_m R_f$ proportional to this current is fed back to the control amplifier (Fig. 7). We have analyzed this system in some detail with the simplifying assumptions that the amplifiers are ideal operational amplifiers with zero output and infinite input impedance and neglecting the effects of the electrodes. We shall only make a few general comments here. Say that the control amplifier A_c (Fig 2) has a transfer function $Y_{opc}(s) =$

[55] L. B. Cohen and B. M. Salzberg, *Rev. Physiol., Biochem. Pharmacol.* **83**, 35 (1978).

[56] B. M. Salzberg, F. Bezanilla, and H. V. Davila, *Biophys. J.* **33**, 90a (1981).

[57] R. Levis, personal communication.

$v_{out}(s)/v_{in}(s)$ where $v(s) = \int_0^\infty V(t)e^{-st}\,dt$ is the Laplace transform of $V(t)$. Similarly, the transfer functions of amplifiers A_D (Fig. 2) and A_5 (Fig. 7) are Y_V and Y_I, respectively, and the admittance of the membrane is $Y_M(s)$. Also let $R_s' = R_s + R_{ce}$ (Fig. 2). It is important, even in simple analysis, to consider the effects of the resistance from the input of the current measuring amplifier A_5 to ground through the guard electrodes. Call this R_G, and let $R_f' = R_f R_G/(R_f + R_G)$.

With these definitions we can say that the transfer function for the relation between the membrane potential V_M and the command potential V_{COM} in Fig. 2 or Fig. 4 is a function of the complex variable s which has two zeros and four poles. The behavior of this system is completely determined by the values of the zeros and the poles (see, e.g., D'Azzo and Houpis[58]). We have found that there are always two real poles. The other two poles may be real or complex conjugates. The response to a step in V_{COM} will be a constant (the step introduces another pole at $s = 0$) plus the sum of four exponentials. For absolute stability the real part of any pole must be negative, so the response will be either the sum of a constant and four decreasing exponentials, or the sum of a constant plus two decreasing exponentials plus an exponentially decaying sinusoid.

There are several ways to approach the question of the behavior of the clamp system. One is to consider the frequency dependence of the transfer function and plot the magnitude of $v_M(j\omega)/v_{COM}(j\omega)$ versus $\omega = 2\pi f$, where f is frequency, on double-logarithmic paper. This is often referred to as a Bode diagram, and is particularly useful when one does not have an analytic expression for the system function. For stability the Nyquist approach is particularly useful when it is possible to readily measure the open-loop transfer function frequency characteristics [$H(j\omega)G(j\omega)$, see below]. For an analytical expression, stability can be determined with the use of the Routh criterion for the presence of positive real parts of the roots of the denominator. We have done this, but the most useful for us seems to be the so-called root locus procedure. (All of the above are well discussed in D'Azzo and Houpis.[58])

If we look at the distribution of the poles and zeros of the transfer function on the s plane and how they move when some parameter of the system is varied, we can observe the complete behavior of the system and obtain clues as to what one can do by adding more poles and zeros to improve it (i.e., with compensating networks). The major difficulty with this approach has always been the necessity of obtaining the complex roots of the denominator of the transfer function. For the simplified version we are considering there

[58] J. J. D'Azzo and C. H. Houpis. "Feedback Control System Analysis and Synthesis." McGraw-Hill, New York, 1966.

are four such roots. If the electrode impedances are included, as well as the compensation introduced by the elements in the feedback across and the input to the control amplifier (Fig. 7), there are seven roots to obtain. The availability of modern computers has changed this picture drastically, and such analyses are becoming feasible.

The term "stability" is used in more than one sense. Absolute stability refers to the situation in which there are no positive real parts of any pole and the system does not go to infinity with time. If the poles are all real and negative, the response is a sum of exponentials and there are no damped oscillations. This is a relative stability often referred to as critical damping. The stability of the system we are considering here depends very much on the bandwidths of the amplifiers employed, relative to the time constant of the membrane being clamped. For very wide-bandwidth amplifiers the system is unlikely to be stable for $R_s = 0$. For infinitely wide bandwidths with $R_s > 0$ the system may be stable, but no negative-resistance compensation is possible. On the other hand, it is quite possible to arrange things so that one can compensate for many times the series resistance. It is intuitively reasonable (and analytically true) that if the clamp system is slow, then only the low frequencies are involved and the presence of the capacitor in the membrane equivalent circuit will have very little effect; one could then compensate for $R_m + R_s$. If the time-constant of the amplifiers is $\tau_0 = 1/\omega_0$, one can compensate up to near $R_s + R_m/(1 + \omega_0^2 R_m^2 C^2)$.[59] For a usual case with the dc gain of the amplifiers equal to 10^5 and ω_0 equal to 2×10^7, the system is unstable for $R_s = 0$. If A is only 10^3 and $R_s = 5\,\Omega\,\text{cm}^2$, one can compensate for about twice R_s without instability.

One reason for the complexity of the analyses of clamp behavior is that the membrane for which one is attempting to control the potential is part of the feedback and not just a load as one finds in most textbooks. With the above definitions for our simplified system, it can be shown that the transfer function can be put into the standard form

$$v_M(s)/v_{COM}(s) = G(s)/[1 + G(s)H(s)]$$

if we let

$$G(s) = -\tfrac{1}{3}Y_{opc}(s)/\{1 + Y_M[R'_s + R'_f(1 - Y_I)]\}$$

and

$$H(s) = Y_V(1 + R_s Y_M) - Y_I \alpha R_f Y_M.$$

This is shown diagrammatically in Fig. 8. The open-loop transfer function is $H(s)G(s)$ and is the function that would be used for the Nyquist diagram approach to stability.

[59] R. E. Taylor and F. Bezanilla, *Program Abstr. Soc. Neurosci.*, p. 306 (1973).

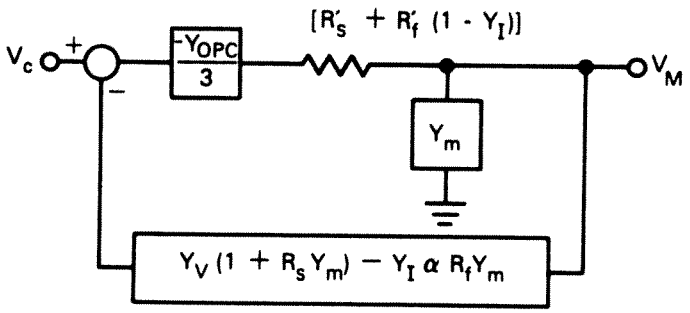

FIG. 8. Equivalent circuit for the transfer function $v_M(s)/v_{COM}(s)$ for the system shown in Fig. 2 with the addition of negative-resistance compensation as shown in Fig. 7. Here $V_c = v_{COM}$; Y_{OPC} is the transfer function of amplifier A_c (Fig. 2); Y_M is the admittance of the membrane with potential V_M; Y_V and Y_I are the total transfer functions of the voltage and current measuring arrangements: R'_s is the sum of the series resistance R_s and the access resistance R_{ce} (Fig. 2); αR_f is the amount of negative-resistance feedback (Fig. 7), where R_f is the feedback resistance of the current measuring amplifier A_5. $R'_f = R_f R_G/(R_f + R_G)$ where R_G is the resistance from the input of A5 to ground (not shown). The compensating networks R_V, C_V and R_I, C_I shown in Fig. 7 are not included here.

10.3.6. Pulse Generation and Data Acquisition

We now describe the basics of an electrophysiological setup used to study ionic and gating currents.

The setup contains (i) a unit to produce the pulse patterns to drive the membrane potential, (ii) voltage clamp electronics to control the membrane potential, (iii) a current measuring amplifier, and (iv) a data acquisition device to store currents obtained for the imposed membrane potentials. The different units of the setup can be easily assembled with conventional pulse generators, oscilloscope, and cameras, but digital computers are obtained at such reasonable prices today that the setup can best be assembled with a computer as the core block.

The description is then that of a particular computer-based system we have used successfully in our laboratory, although many similar systems have been used by many other investigators for many years.[60–62]

Basically, the computer is used to produce the pulse patterns used to drive the membrane potential and also to acquire and store the membrane currents. The computer, a Data General Nova 3 (Southboro, Ma) is programmed in a combination of FORTRAN IV and ASSEMBLER languages. ASSEMBLER is used to handle all the peripherals or input/output instructions and also in portions of the program when the FORTRAN execution times are excessively long.

[60] B. Hille, Ph.D. Thesis, Rockefeller University, New York, 1967, [University Microfilms (No. 68-9, 584), Ann Arbor, Michigan].

[61] C. M. Armstrong and F. Bezanilla, *Ann. N.Y. Acad. Sci.* **264**, 265 (1975).

[62] W. Nonner, E. Rojas, and R. Stämpfli, *Pfluegers Arch.* **354** 1 (1975).

10.3.6.1. Pulse Generation. The operator assembles the pulse pattern, and the program stores the sequence of amplitudes and durations in a bank of random-access memories. The random-access memories are communicated to a digital-to-analog (D/A) converter. Communication between the memories and the D/A converter takes place via optical isolators to prevent ground loops and, consequently, to decrease the pickup of digital noise in the analog side of the setup. The output of the D/A converter contains the pulse patterns, as decided by the investigator, and is applied as the command signal of the voltage clamp circuit. Most often the pattern is a series of rectangular pulses, but ramps[33,63] and other waveforms are sometimes employed.[64]

10.3.6.2. Data Acquisition. The membrane current is amplified and filtered conveniently to cover the dynamic range and speed of the sample and hold amplifier preceding the analog-to-digital (A/D) converter that digitizes the signal to be entered into the computer memory. Data from the A/D converter are transferred by way of optical isolators to the computer memory via the "data channel" or direct memory access (DMA); data transfer is not under direct program control, having the highest priority in the computer cycle operation. The stored current signal may or may not be processed before it is stored in hard or flexible magnetic disk.

An important design consideration in this setup is a clear separation between the analog and digital sections of the instruments. We have found that unless the computer is physically separated from the experimental table, significant digital noise is picked up by the analog circuitry, with adverse effect on the signal-to-noise ratio. In practice, the voltage clamp and current amplifier are set on or very near the experimental chamber. The D/A converter used to generate the voltage pulses is fed with its own power supply, and the same is done with the multiplexer, sample and hold, and A/D converter used to enter data into the computer. Both A/D and D/A converters are connected to the computer with multiple twisted pair cables. The analog signals, voltage, and current, are displayed in an oscilloscope different from the oscilloscope used to display data stored in the computer.

10.3.6.3. Instrumentation and Recording of Gating Currents. The use of a computer to generate the command pulses in a voltage clamp system is especially useful in the detection of gating currents. Gating currents are displacement currents produced by the movement of charge *inside* the membrane that are thought to be related to the opening and closing of the ionic channels.[18b,65] (for a review, see Almers[66]). The currents are

[63] H. M. Fishman, *Nature (London)* **224**, 1116 (1969).

[64] Y. Palti and W. J. Adelman, Jr., *J. Membr. Biol.* **1**, 431 (1969).

[65] R. D. Keynes and E. Rojas, *J. Physiol. (London)* **239**, 393 (1974).

[66] W. Almers, *Rev. Physiol., Biochem. Pharmacol.* **82**, 96 (1978).

voltage and time dependent, and the method used to separate them from the larger capacitive currents is based on their nonlinear dependence on voltage. The first method ($\pm P$ procedure) used to detect them consisted of recording the membrane current for equal-magnitude but opposite-polarity pulses and adding the resultant currents. With the computer, it is an easy task to generate a sequence of positive (test) and negative (subtracting) pulses very well matched in amplitude and time course if the D/A converter has a resolution of 1 part in 4096 (12 bits). (The main problem is, however, to reduce the "glitches" to an acceptable minimum.) It was soon found that to measure gating currents more accurately, the subtracting pulse had to be started from a more hyperpolarized potential. Because strongly negative potentials can have deleterious effects on the membrane, the "$\frac{1}{4}P$" procedure was devised.[61,67] In this technique a test pulse of amplitude P is given, followed by four pulses of amplitude $\frac{1}{4}P$ riding on a very negative or very positive potential. Again, the computer can generate the sequence and amplitude of the pulses with a high degree of accuracy. Besides, the program can be made flexible enough to accommodate the "$\pm P$," "$\frac{1}{4}P$" procedures, or any other combination. When the $\pm P$ procedure is used, the currents are added; in the $\frac{1}{4}P$ procedure the currents from the four small pulses are added, and the result is subtracted from the current produced by the test pulse. With the computer it is quite simple to process the currents recorded, because under program control the current produced by each pulse can be stored and later added to or subtracted from the others. Furthermore, it is a normal procedure to signal-average the currents recorded to improve the signal-to-noise ratio; again, this procedure can be implemented with the computer with the same program that generates pulse amplitudes, durations, and sequences, and records the membrane currents.

The high gain required to record gating currents may produce saturation of the amplifiers. This problem has been solved by adding to the currents obtained, for both test and subtracting pulses, the current produced by a passive network which mimics the linear part of the membrane response.[67] If this transient generator is itself highly linear, the exact form produced is of no importance because it will be eliminated by the subtraction procedure.

10.3.6.4. Instrumentation for Studying Noise and Single Channels. The studies of membrane channel noise and single-channel current fluctuations have contributed precise values for the conductances of transmembrane ionic channels. As well as providing the most tangible proof of the existance of discrete molecular channels, the noise and channel-jump experiments provide unique insights into the kinetics of gating. Membrane noise analysis has by now become a large enterprise which has

[67] F. Bezanilla and C. M. Armstrong, *J. Gen. Physiol.* **70**, 549 (1977).

been reviewed extensively.[68–68e] Two of the main considerations in this important area of research are how to extract the noise spectrum generated by the activation of ionic channels from other extraneous sources of noise generated in a voltage-clamped preparation, and how to interpret the observed noise spectrum in terms of appropriate stochastic models of the gating process.

Single-channel currents observable with an isolated small (of the order of 1 μm^2 in area) patch of membrane are the ultimate in resolution for membrane currents. The major considerations for this technique are how to fabricate electrodes which can be pressed up against the cell surface to make a seal and how to construct sufficiently low-noise virtual-ground current detectors for the picoampere-level currents involved. These techniques are presented in three excellent reviews by Neher and his collaborators.[68f–68h]

10.4. Voltage Clamp with Microelectrodes

10.4.1. Two Microelectrodes

In principle, it is possible to control the membrane potential using two intracellular electrodes, one to measure potential and the other to inject current. The technique, however, has two serious drawbacks: (i) it does not provide space clamp, and (ii) the high resistance of the microelectrodes make the system inherently slow.

The high resistance of the microelectrodes is in some cases not a serious problem. For example, the two-microelectrode technique has been used to voltage-clamp the end-plate potential in the frog neuromuscular junction.[69] Since in this preparation the end plate is usually activated by stimulation of the presynaptic terminal or by direct microiontophoresis of transmitter

[68] L. J. DeFelice, *Int. Rev. Neurobiol.* **20**, 169 (1977).

[68a] L. J. DeFelice, "Introduction to Membrane Noise." Plenum, New York, 1981.

[68b] V. E. Dionne, *in* "Techniques in Cellular Physiology" (P. F. Baker, ed.), in press. Elsevier, North-Holland, New York, 1982.

[68c] H. Lecar and F. Sachs, *in* "Excitable Cells in Tissue Culture" (P. G. Nelson and M. Lieberman, eds.), p. 137. Plenum, New York, 1981.

[68d] E. Neher and C. F. Stevens, *Ann. Rev. Biophys. Bioeng.* **6**, 345 (1977).

[68e] F. Conti and E. Wanke, *Q. Rev. Biophys.* **8**, 451 (1975).

[68f] E. Neher, B. Sakmann, and J. H. Steinbach, *Pfluegers Arch.* **375**, 219 (1978).

[68g] E. Neher, *in* "Techniques in Cellular Physiology" (P. F. Baker, ed.), in press. Elsevier North-Holland, New York, 1982.

[68h] O. P. Hamill, A. Marty, E. Neher, B. Sakmann, and F. J. Sigworth, *Pfluegers Arch.* **391**, 85 (1981).

[69] A. Takeuchi and N. Takeuchi, *J. Neurophysiol.* **22**, 395 (1959).

substance at constant potential, there is no need to charge the membrane capacity at high speed. In some other applications, when it is necessary to control the membrane potential in a small region but the recording of the current is not important, two-microelectrode voltage clamps have been used successfully (see, for example, Adrian *et al.*[70]).

However, the usual application of the voltage clamp to study the current–voltage characteristics of the membrane is a problem which requires special attention and varies with the type of cell considered because the potential distribution depends on the cable properties of the cell, which are partially related to its geometry.

To consider the problems in probably one of the worst cases, let us assume that we wish to voltage clamp a long cylindrical cell with two microelectrodes as was briefly discussed at the beginning of this article. The membrane current will be measured as the total current injected by the current microelectrodes. The potential at the tip of the voltage microelectrode will be controlled by the feedback circuitry, but the potential in other regions of the fiber will be given by the potential distribution in a long cylinder. In particular, in the steady state and assuming that the conductances are independent of voltage (not a very interesting case but useful for illustrative purposes), the voltage will be distributed according to $V_0 e^{-x/\lambda}$, where V_0 is the potential at the current injection point and λ is the space constant. It is easy to see that in the case of length long compared to λ, the current measured will not correspond to the membrane current in the controlled patch of membrane, but will be a mixture of the currents of different membrane patches all at different membrane potentials. For example, the length of a frog sartorius muscle fiber is about 20 times the space constant at rest, making it inappropriate for two-microelectrode voltage clamping. This situation is acceptable if the variation of the membrane potential with distance is negligible, a condition that can be approximated in two common cases: the short cylindrical cell and the spherical cell.

10.4.1.1. The Short Cylindrical Cell. It is intuitively clear that a short fiber will show less potential variation along its length the shorter it is in comparison to its length constant λ. Weidmann[71] has presented solutions of the distribution of potential in a short cable for the steady-state case. It can be easily shown that the potential distribution will be more homogeneous when the control of membrane potential is done in the center rather than at the end of the fiber.

To get an idea of the homogeneity of potential control, we show the prediction made by the solution of the cable equation for the case of a short

[70] R. H. Adrian, W. K. Chandler, and A. L. Hodgkin, *J. Physiol.* **204**, 207 (1969).
[71] S. Weidmann, *J. Physiol.* (*London*) **118**, 348 (1952).

cable of length $2l$ with both ends open circuited and with potential control at the center of the fiber.

The equation to be solved is (e.g., Taylor[5])

$$\lambda^2 \frac{\partial^2 V}{\partial x^2} - \tau \frac{\partial V}{\partial t} - V = 0, \tag{10.4.1}$$

where x is the distance measured from the center to *either* end; V is the membrane voltage, t is time, λ is the space constant equal to $\sqrt{r_m/r_i}$; τ is the membrane time constant equal to $r_m C_m$; and r_i, r_m, and C_m are the internal resistance, membrane resistance, and membrane capacitance for unit length, respectively.

The boundary conditions at the ends require no current circulation:

$$i(x = l) = \frac{1}{r_i} \frac{\partial V}{\partial x}\bigg|_{x=l} = 0. \tag{10.4.2}$$

At the center, the membrane potential is set equal to V_{COM}, and the total current injected I_0 is divided equally into the two segments of length l (total fiber length is $2l$). The solution of the above equations for V_{COM}, an arbitrary function of voltage $V_{COM} = f(t)$, was obtained by the use of the Laplace transform, the complex inversion formula, and the convolution theorem, giving

$$V(x, t) = \frac{\pi\lambda^2}{l^2\tau} \sum_{n=1}^{\infty} (-1)^n (2n - 1) \cos \frac{(2n - 1)\pi(l - x)}{2l} \times \int_0^t f(t - z) \exp\left[\frac{-z}{\tau}\left(\frac{\pi^2(2n - 1)^2\lambda^2}{4l^2}\right)\right] dz. \tag{10.4.3}$$

Several driving functions can be analyzed with this equation. The most obvious case is the step function: $f = 0$ for $t < 0$ and $f = V_0$ for $t \geq 0$. In this case the distribution is given by (see also Waltman[72])

$$V(x, t) = V_0\left(\frac{\cosh[(l - x)/\lambda]}{\cosh(l/\lambda)} - 4\pi \sum_{n=1}^{\infty} \frac{(-1)^{n+1}(2n - 1) \exp\{-(t/\tau)[\pi^2(2n - 1)^2\lambda^2/4l^2 + 1]\} \times \cos[(2n - 1)\pi(l - x)/2l]}{4l^2/\lambda^2 + \pi^2(2n - 1)^2}\right). \tag{10.4.4}$$

Figure 9 shows an example of $V(x, t)$ when $l/\lambda = 0.44$. It is clear that the potential rises at the ends more slowly than at the center, and at long times

[72] B. Waltman, *Acta Physiol. Scand.* **66**, Suppl. 264 (1966).

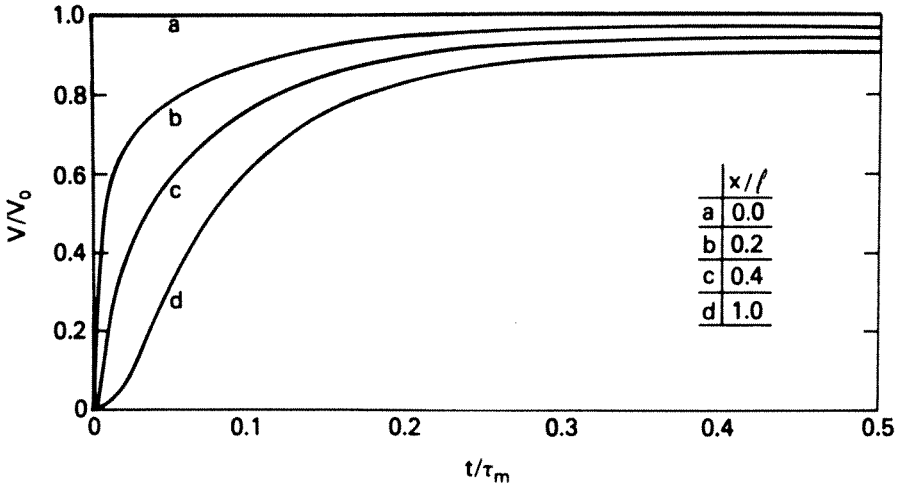

FIG. 9. Normalized membrane potential as a function of time in a voltage-clamped short fiber. At $x = 0$ (center of the fiber) a step function of voltage of magnitude V_0 is applied (curve a) and at distances x/l of 0.2 (curve b), 0.4 (curve c), and 1.0 (curve d); the potential is plotted as a function of time. Abscissa is normalized time t/τ, with τ the membrane time constant. Ordinate is normalized membrane potential defined as the membrane potential divided by the controlled potential V_0. λ is the space constant, and l/λ was taken as 0.44. Curves computed with Equation (10.4.4).

the potential at the ends is different from the potential at the center. The parameters used in Fig. 9 were obtained from experimental measurements performed in the lumbricalis muscle of digiti IV of the frog.[73] When a third microelectrode was inserted at the end of a voltage-clamped fiber, a very similar voltage waveform as observed in Fig. 9 was recorded.[74,74a]

It is interesting to compare the current predicted by the above model with the current expected for the case in which there is no decrement along the fiber. The total current I_0 injected by the current microelectrode is given by

$$I_0 = \frac{2V_0}{r_i}\left\{\frac{\tanh(l/\lambda)}{\lambda} + \frac{4\pi^2}{l}\sum_{n=1}^{\infty}\frac{(2n-1)^2}{4l^2/\lambda^2 + \pi^2(2n-1)^2} \times \exp\left[-\frac{t}{\tau}\left(\frac{\pi^2(2n-1)^2\lambda^2}{4l^2}\right)\right]\right\}. \tag{10.4.5}$$

If one analyzes the ideal case in which $r_i = 0$ (perfect space clamp) the total current is given by

$$I_0 = 2V_0 l/r_m, \quad t > 0. \tag{10.4.6}$$

[73] F. Bezanilla, C. Caputo, and P. Horowicz, *Acta Cient. Venez.* **22**, Suppl. 2, 72 (1971).
[74] P. Heistracher and C. C. Hunt, *J. Physiol. (London)* **201**, 589 (1969).
[74a] F. Bezanilla, C. Caputo, and P. Horowicz, personal communication.

$I_0 \to \infty$ at $t = 0$, and $I_0 = 0$ at $t < 0$. It should be noted that Eq. (10.4.5) approaches (10.4.6) when $r_i \to 0$. The current measured in a typical two-microelectrode clamp is the total current I_0, and from the above discussion it is clear that it will not represent the properties of a single patch of the membrane under study, but instead the charging of the distributed membrane capacitance. The case approaches ideality when the space constant is very large compared to the length of the fiber. The error can be computed with Eqs. (10.4.5) and (10.4.6). If the length and diameter of the cell are known, it is possible to roughly estimate whether two-microelectrode clamping could be used. The value of λ is given as

$$\lambda = \sqrt{r_m/r_i} = \sqrt{R_m \pi a^2 / 2\pi a R_i} = \sqrt{R_m a / 2R_i},$$

where a is the radius, R_m is the specific membrane resistance ($\Omega\,\text{cm}^2$); and R_i is the resistivity of the internal medium (Ω cm). We can approximate λ to

$$\lambda \approx \sqrt{20a} \quad \text{(cm)}$$

for typical average values of R_m and R_i. For an appropriate space clamp with two microelectrodes, l/λ should be less than or equal to 1, and using the above approximation the length of the fiber should be

$$l \leq \sqrt{20a}.$$

It should be noted, however, that the theoretical expressions presented above have been obtained with a simple core-conductor model which does not take into account current spread in three dimensions. Three-dimensional considerations are important near the site of current injection, and this may lead to error in the controlled potential at the tip of the voltage electrode when both electrodes are very close together.[75] It is also known that when the radius a of the fiber approaches λ, the three-dimensional equation should be used instead.[75] It is probably not appropriate to discuss that case in any detail because when $a \approx \lambda$ the space clamp will be a complete failure, as can be seen from the previous equations, unless $l \approx a$, in which case we are approaching the case of the spherical cell.

10.4.1.2. The Spherical Cell. In the approximation of the core-conductor model made in the previous paragraph, the spherical cell would be considered an ideal case. We can test the validity of the assumption of potential uniformity by approaching the problem in the three-dimensional case. The solution to the problem of a spherical cell with two microelectrodes, one to inject current and the other to record potential, has been presented

[75] R. S. Eisenberg and E. A. Johnson, *Prog. Biophys. Mol. Biol.* **20**, 1 (1970).

in detail by Eisenberg and Engel,[76] Peskoff and Eisenberg,[77] and Peskoff and Ramirez.[78] Although their solution has not been produced for voltage clamp, we can assume that their voltage electrode is in our case the site of membrane potential control, and then ask for the potential in other places of the cell, without moving the current electrode and without changing the injected current, that will maintain the controlled potential in the original position. It should be noted that in the derivation by Eisenberg and Engel,[76] the current source was assumed ideal, that is, of infinite impedance. This is true in the case of "current clamping" because the electronics in that case are designed to have very high-impedance current electrode. When the objective is voltage clamping, the electrode resistance is made low purposely to be able to inject as much current as needed to control the membrane potential in the shortest possible time. However, a very low source resistance cannot be obtained because in practice the minimum resistance is given by the current microelectrode, which typically will vary between 5 and 100 MΩ. In any case, the problem discussed by Eisenberg and Engel[76] can be applied without modifications for the steady state because the impedance of the current source is not important provided the amount of current it supplies is known. In the transient solution, the situation is more involved, and it has not been treated in a form convenient for the discussion of the voltage clamp.

Let us consider the steady-state situation. Using Eqs. (1) and (2) of Eisenberg and Engel[76] we find that the potential distribution $V_m(\theta)$ is given by

$$V_m(\theta) = (I_0 R_m/4\pi b^2) f(\theta, b/\Lambda),$$

where θ is the angular separation between the current and voltage electrode; b is the radius; Λ is the space constant, equal to R_m/R_i with R_m membrane resistance per unit area ($\Omega\,\text{cm}^2$) and R_i internal resistivity ($\Omega\,\text{cm}$); and I_0 is the total injected current. If the potential is homogeneous in the cell surface, it is given by

$$V_0 = I_0 R_m/4\pi b^2,$$

whence it is clear that the factor $f(\theta, b/\Lambda)$ is defined as

$$f(\theta, b/\Lambda) = V_m(\theta)/V_0.$$

The situation sought in voltage-clamping a spherical cell is a minimum variation of potential with angle separation. It must be remembered that during voltage clamping the potential will be controlled at the voltage electrode; therefore, we must ask what is the deviation from a constant membrane potential with any angle between current and voltage electrode.

[76] R. S. Eisenberg and E. Engel, *J. Gen. Physiol.* **55**, 736 (1970).
[77] A. Peskoff and R. S. Eisenberg, *J. Math. Biol.* **2**, 277 (1975).
[78] A. Peskoff and D. M. Ramirez, *J. Math. Biol.* **2**, 301 (1975).

Eisenberg and Engel (Ref. 76, Table II) have published a table of $f(\theta, b/\Lambda)$ as a function of angle θ and the ratio b/Λ. It must be emphasized that in the vicinity of the current electrode there is a steep rise in membrane potential, but for most of the cell (for example, angles larger that 20°, and $b/\Lambda < 0.01$), the variation in membrane potential will be less than 5%. This is not very difficult to achieve because a cell 100 μm in diameter with a membrane resistance of 5 kΩ cm^2 and an internal resistivity of 100 Ω cm will have $b/\Lambda = 0.0001$. This value could be reduced 100 times (for example, during excitation) and still result in a potential distribution with less than 5% variation for angles larger than 20°. It should be noted, however, that a variation of 5% could produce local circuit currents near the threshold region for a very steep conductance versus voltage curve and, consequently, produce a total current that would be practically impossible to interpret in terms of the properties of an elementary membrane patch.

The above analysis assumes that the electrodes are inserted just under the membrane surface and that the external medium is isopotential. The first assumption is reasonable in the majority of the cases because it is not desirable to introduce the tip of the electrode too deep to prevent cell damage. In very small cells, however, this assumption may not be valid. The external isopotentiality has been demonstrated to be a very good approximation by Peskoff and Eisenberg,[77] who examined the difference it would make in their solution by including a finite conductivity of the external solution.

The discussions about space clamping in two-microelectrode arrangements have been limited to the case where the system is linear. In practice, the most interesting preparations will have conductances which are dependent on membrane potential; consequently, the above equations are not directly applicable. However, some insight can be obtained by changing the membrane parameters in the steady-state situation. The situation is even more difficult when regenerative phenomena are present because voltage-dependent negative conductances are involved and, in general, numerical solutions are required to analyze each particular case. Complications arise when the spherical cell has dendrites or axons, because current will be drained into cablelike structures, sometimes excitable, which could result in very large nonuniformities.

Having examined the problem of space clamp when voltage clamping with two microelectrodes, let us consider now the limitations imposed by the use of micropipettes. Microelectrodes are made by pulling glass tubing, leaving tips less than 1 μm in diameter, which are then filled with a concentrated electrolyte solution. Normally, electrodes to record membrane potential are filled with 3 *M* KCl. Electrodes to pass current are normally not filled with KCl because they cannot pass enough current for most applications; it has been found that electrodes filled with 2 *M* K-Citrate exhibit lower resistance to current injection. Because of the small diameter near

the tip, the resistance of these electrodes ranges between 5 and 500 MΩ depending on tip diameter, shank shape, and the electrolyte filling them. The high resistance of microelectrodes imposes serious limitations on the implementation of a voltage clamp system. Voltage recording must be done with very high-input-impedance amplifiers so that the electrode–amplifier combination does not drain current from the cell. The distributed capacitance of the wall of the microelectrode, the electrical shield, and the input capacitance of the amplifier, together with the high resistance of the pipette, constitute a low-pass filter that gives an erroneous measurement of the actual membrane potential when varying with time. The approach commonly used to solve this problem is to electronically compensate for the input capacitance using positive feedback through a capacitor (e.g., Bak[79]). The adjustment of the compensation is not a simple matter (for a discussion of methods, see Moore[21]), and as some of the capacitance is distributed, it cannot be compensated. Although the result is a faster response than the case without capacity compensation, the transfer function of the amplifier introduces phase lags that are important in the overall performance and stability of the voltage clamp feedback circuit. To decrease the need for negative capacity compensation, "driven shields" have been used which consist of connecting the shields at the input to the output of the amplifier. As the output is a low-impedance point with respect to ground, it shields effectively, and being at the same potential as the shielded conductor (the input), the capacity of the shield does not need to be charged or discharged when the potential of the microelectrode changes.

A very ingenious way to decrease the influence of the electrode capacitance has been devised by Eisenberg and Gage[80] based on the idea of bringing the interior of the cell to virtual ground.[81] In this arrangement a high-input-impedance operational amplifier is used, the microelectrode is connected directly to the inverting input, the output of the amplifier is connected to the bath. As the positive input of the amplifier is grounded, the negative input will be at "virtual" ground, and the output will be at minus the membrane potential. That is, measuring the potential in the bath with respect to ground gives the cell membrane potential. Meanwhile, all the effects of capacity to ground have been eliminated because the electrode is at ground potential, and only the capacitance across that portion of the wall of the microelectrode in the bathing solution remains, which can be reduced significantly, lowering the level of the external solutions. This configuration is recommended for measuring membrane potential, especially when used as part of the feedback loop in a voltage clamp system.

[79] A. F. Bak, *Electroencephalogr. Clin. Neurophysiol.* **10**, 745 (1958).
[80] R. S. Eisenberg and P. W. Gage, *J. Gen. Physiol.* **53**, 279 (1969).
[81] B. Frankenhauser, *J. Physiol. (London)* **135**, 550 (1957).

The current electrode also has a high resistance which imposes problems in the design of the voltage clamp. It has been found that to inject enough current to charge the membrane capacitance following a step change in voltage, a high-voltage amplifier is required because the high resistance of the pipette effectively limits the amount of current to be passed. Some investigators have used the internal amplifier of the oscilloscope,[82] and others have used operational amplifiers with large output-voltage range.[74]

However, even the use of high-voltage control amplifiers does not solve the problem of speed encountered when the membrane capacitance is charged through a large resistor. Katz and Schwartz[22] have proposed a compensating network for reducing the effect of the access resistance as discussed in Section 10.3.5.3. If the amplifier had infinite gain at all frequencies, it would be possible to impose a fast rise in potential across the membrane, but the limited bandwidth and slow rate of practical amplifiers limit even further the speed of the voltage clamp system.

The interaction ("cross talk") between the voltage and current electrodes due to capacitative coupling between them is important during fast transients, because it introduces undesired transients in the voltage clamp feedback circuit which may render it unstable. The coupling can be effectively reduced by positioning a shield between the electrodes and impaling the cell with a wide angle between them.

10.4.2. Three Microelectrodes

Adrian *et al.*[83] devised a technique to control the membrane potential of a muscle fiber and measure the current in the neighborhood of the controlled region. Their technique is based on the fact that membrane current is roughly proportional to the voltage gradient along the fiber. They impaled three microelectrodes near the natural end of a fiber, and, controlling the potential at the electrode closer to the end (control electrode) by passing current through the electrode farthest from the end, they measured the membrane current as the potential difference between the central electrode and the control electrode. Using the linear cable equation, they derived the exact expression for the current as a function of the potential difference between the two electrodes, and they found that if l/λ is less than 2, the error is less than 5%, if the current is measured just as the potential difference between the electrodes (l is the distance between the end of the fiber and the control electrode and between the two voltage electrodes, λ is the space constant). The method works very well to measure delayed rectification, but fails in the range of potentials needed to measure the sodium current. The reader is

[82] L. L. Costantin, *J. Physiol.* (*London*) **195**, 119 (1968).

[83] R. H. Adrian, W. K. Chandler, and A. L. Hodgkin, *J. Physiol.* (*London*) **208**, 607 (1970).

referred to the original paper for details of the sources of the errors of this technique.[83] Kootsey[84] has calculated the errors of this technique using numerical procedures for the case of negative conductance and has found that $l/\lambda = 2$ produces unacceptable errors. The error decreases to small but still noticeable values when $l/\lambda = 0.86$.

Recently, the technique of making the interior of the fiber virtual ground has been applied to the three-microelectrode voltage clamp.[84a]

10.5. Voltage Clamp of an Isolated Patch Using External Pipettes

The smaller the region in which the membrane current is measured, the closer one gets to the ideal situation of recording current from an isopotential region. In this chapter we review briefly some of the attempts that have been made to isolate a small patch of surface membrane using external pipettes to record the current through it.

10.5.1. External Patch Isolation

Strickholm[85,86] manufactured fire-polished pipettes and applied them to the surface of skeletal muscle fibers of the frog. He relied on the fact that the leakage conductance produced by imperfect contact with the membrane was much larger than the membrane conductance of the patch, and with this the patch of external surface membrane may be considered to be "clamped" at a constant potential. However, the lack of a feedback circuit to hold the patch voltage controlled when the patch conductance changed made this arrangement of limited value.

A significant improvement was made by Frank and Tauc.[87] These authors used two internal microelectrodes to voltage-clamp the membrane potential of a mollusk neuronal body and brought an external pipette near the external surface of the soma. The interior of this pipette was connected to the input of an operational amplifier connected in the current-to-voltage configuration. The other input of the amplifier was connected to the bath, making the output of the amplifier proportional to the current flowing through the patch

[84] J. M. Kootsey, *Fed. Proc. Fed. Am. Soc. Exp. Biol.* **34**, 1343 (1975).

[84a] P. C. Vaughan, J. G. Mclarnan, and D. D. F. Loo, *Can. J. Physiol. Pharmacol.* **58**, 999 (1980).

[85] A. Strickholm, *J. Gen. Physiol.* **44**, 1073 (1961).

[86] A. Strickholm, *J. Cell. Comp. Physiol.* **60**, 149 (1962).

[87] K. Frank and L. Tauc, *in* "Cellular Function of Membrane Transport" (S. Hoffman, (ed.), Prentice-Hall, Englewood Cliffs, New Jersey, 1963.

under the pipette tip. The comparison between total current and current through the patch revealed that the total current had contributions from the axonal membrane which was not under voltage control. The patch revealed current patterns that increased smoothly with membrane depolarization as was expected from a well-controlled membrane patch.

A further improvement was made by Neher and Lux[88] when they incorporated a feedback loop in the extracellular pipette using a partitioned pipette, one half to measure the pipette potential and the other to inject current. In their arrangement, the potential *inside* the pipette was maintained at bath potential by means of a feedback circuit. The current needed to control the potential of the pipette was measured as the current through the patch, the cell membrane potential still being controlled by an independent feedback circuit with two microelectrodes. Using feedback in the extracellular pipette effectively decreases the access resistance (pipette resistance) to the input of the amplifier, decreasing significantly the effect of the shunt resistance produced by the leakage pathway between the pipette wall and the cell surface.

The original approach of Strickholm using the extracellular pipette to control the membrane potential of the patch of membrane under the pipette was notably improved by Fishman.[89] He made a double-barreled concentric pipette, the internal to measure patch voltage and to inject current, and the external to introduce sucrose to improve the seal of the pipette against the membrane. As the preparation used was the squid giant axon, which is surrounded by a coat of Schwann cells and connective tissue, the sucrose was essential to decrease the leakage under the walls of the central pipette. Even with the sucrose flow the seal resistance was of the order of 2 MΩ, which is about ten times smaller than the membrane resistance under the pipette. The voltage clamp was established as a feedback circuit to control the potential inside the pipette at a predetermined voltage, and the current needed to maintain this potential was considered to be the current of the membrane patch under the pipette plus the leakage current due to the imperfect seal. This latter current could be subtracted off electronically because it was found that the leakage resistance was ohmic. The membrane currents recorded by Fishman resemble the current recorded with the conventional axial-wire technique, and he provided tests for isopotentiality inside the axon by inserting a voltage measuring pipette. This technique has been used to record membrane noise taking advantage of the fact that the currents are measured from a small patch of membrane.[90]

[88] E. Neher and H. D. Lux, *Pfluegers Arch.* **311**, 272 (1969).

[89] H. M. Fishman, *J. Membr. Biol.* **24**, 265 (1975).

[90] H. M. Fishman, D. J. M. Poussart, and L. E. Moore, *J. Membr. Biol.* **24**, 281 (1975).

The isolation of a patch of membrane with an external pipette has been perfected by Neher and Sakmann[40] and Neher *et al.*[68f] By using collagenase-treated denervated muscle fibers, the seal resistance was increased up to 50 MΩ, and they were able to record the opening and closing of single postsynaptic channels. In their arrangement an extremely low-noise operational amplifier was used as a current-to-voltage converter with its input connected to the pipette. Using 500 MΩ as a feedback resistor, the main source of noise in that configuration is the input voltage noise of the operational amplifier that appears as a current in the leakage resistance under the seal between the pipette and the cell surface. With 50-MΩ seal resistance the noise was low enough to observe a single acetylcholine-activated channel with a good signal-to-noise ratio.

Recently, Sigworth and Neher[91] and Horn and Patlak[91a] have achieved seal resistances above 1 GΩ using tissue culture cells. Sigworth and Neher have reported fluctuations of single sodium channels. Horn and Patlak have been able to excise a membrane patch attached to the pipette, enabling them to readily change the medium on the inner side of the membrane. These matters, and others, are discussed in recent reviews.[68g,68h]

10.5.2. Internal Access

Several groups of investigators[92–94] have used the external pipette to gain access to the interior of the cell (Fig. 10). Although these techniques are not strictly regarded as patch isolation, we have included them here because they utilize external pipettes (or perforated plastic partitions) that have to be pressed against the membrane to obtain a good seal.

Once the seal is in contact with the pipette, suction is applied to increase seal resistance and if the suction is increased even more, it is possible to break the cell membrane (or break it with a wire inside the pipette) and, consequently, have access to the internal medium (Fig. 10a). Under these conditions when the interior of the pipette is voltage clamped, the whole cell will be voltage clamped. The accuracy in the current recordings will depend on membrane parameters and geometry of the cells as discussed in the section on microelectrode clamping. This technique has the added advantage of making possible the exchange of the internal solution by known solutions loaded and circulated through the pipette shank.

[91] F. J. Sigworth and E. Neher, *Nature (London)* **287**, 447 (1980).
[91a] R. Horn and J. B. Patlak, *Proc. Natl. Acad. Sci. U.S.A.* **77**, 6930 (1980).
[92] P. G. Kostyuk and O. A. Krishtal, *J. Physiol. (London)* **270**, 545 (1977).
[93] K. Takahashi and M. Yoshii, *J. Physiol. (London)* **279**, 519 (1978).
[94] K. S. Lee, N. Akaike, and A. M. Brown, *J. Gen. Physiol.* **71**, 489 (1978).

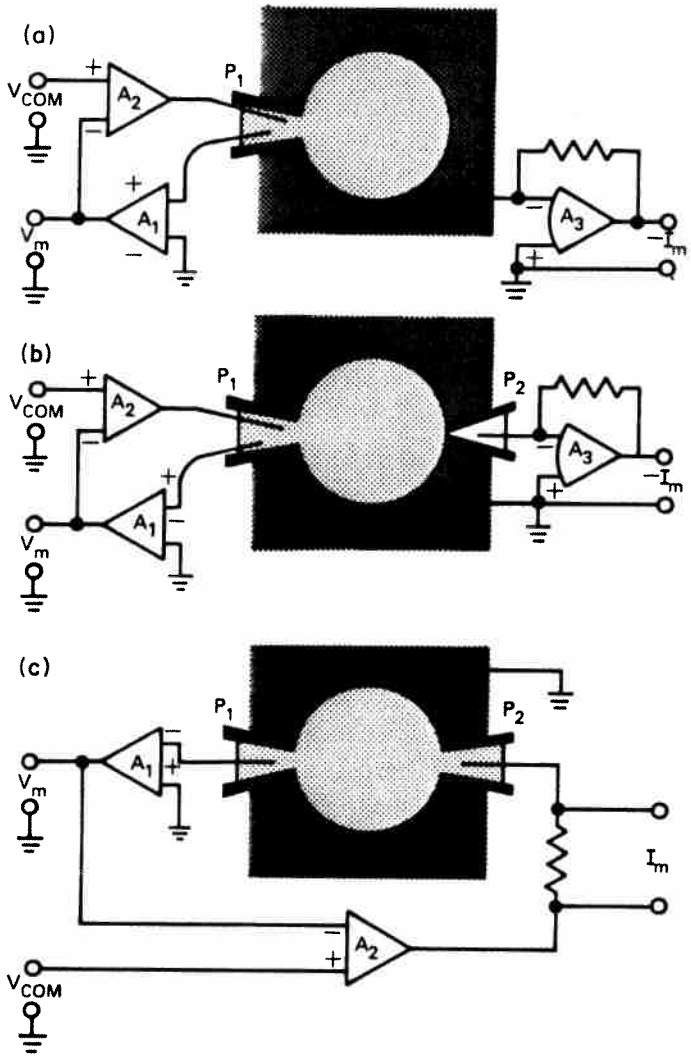

FIG. 10. Schematic diagrams of patch clamps with internal access. (a) Simple pipette arrangement. The interior of pipette P_1 is in direct contact with the cell contents. The voltage clamp circuit (A_1, A_2) controls the internal membrane potential and the total cell current is measured by the current to voltage converter A_3. (b) Voltage clamp as in (A) but current is only measured out of a small membrane patch with the smaller pipette P_2 that is against the *external* surface of the cell.[95] (c) Two pipettes have access to the interior of the cell. P_1 is used to measure the membrane potential with amplifier A_1 and then compared to the command voltage at amplifier A_2 that injects current through pipette P_2. Current I_M is measured as the total current injected into the cell.[96]

Kostyuk *et al.*[95] have carried this technique one step further (Fig. 10b). They have manufactured plastic pipettes that, when applied with suction against a molluscan neuronal soma, resulted in seal resistances of up to $10^9\ \Omega$. They use one pipette to gain access to the cell interior by applying

[95] P. G. Kostyuk, O. A. Krishtal, and V. I. Pidoplichco, *Dokl. Akad. Nauk SSSR* **238**, 478 (1978).

enough suction to break the cell membrane and to voltage clamp the soma. Another pipette with smaller tip diameter is applied to the intact part of the cell soma; enough suction is applied to obtain a good seal, but not enough to rupture the membrane. This second pipette is connected to a current-to-voltage transducer to record the membrane current of the patch isolated under the pipette. With this technique they have been able to record current noise related to calcium channels.

Krishtal[96] has used the same type of pipettes to gain access to the cell interior with two pipettes in the same cell (Fig. 10c). One pipette is used to measure voltage and the other to pass current, approaching an almost ideal situation when the cells are small and have high membrane resistance. This technique makes possible the internal perfusion of the soma, as solution is passed from one pipette to the other removing the contents of the cell.

Conti and Neher[96a] have used an L-shaped pipette on the inside of the squid giant axon to isolate a small patch of membrane and record the fluctuations of single potassium channels.

Recently a new preparation has been described in which a squid axon had been cut open and the resulting membrane sheet positioned in a chamber separating two compartments. Normal-looking ionic and gating currents have been reported from this cut axon,[41] and fluctuations from a few sodium channels have been observed by applying patch pipettes to the internal surface membrane.[96b]

10.6. Voltage Clamp with Gap Isolation Techniques

Some of the most rewarding voltage clamp techniques can be gathered under the heading gap isolation techniques. In this case, cylindrical cells are mounted across partitions and patches of membrane are isolated by means of Vaseline, sucrose, Vaseline–sucrose, or Vaseline–air gaps. Voltage clamping of excitable cells using gap isolation techniques has provided sustained experimental evidence about electrophysiological mechanisms or preparations in which microelectrodes, pipette patch isolation, and axial-wire techniques cannot be used. The methods in general were initially developed for electrical recordings from the naturally isolated patch of excitable membrane in the node of Ranvier, but they have been modified to artificially define a small patch of membrane in unmyelinated nerve axons and muscle fibers.

[96] O. A. Krishtal, *Dokl. Akad. Nauk SSSR* **238**, 482 (1978).
[96a] F. Conti and E. Neher, *Nature (London)* **285**, 140 (1980).
[96b] I. Llano and F. Bezanilla, *Biophys. J.* **37**, 101a (1982).

10.6.1. Node of Ranvier

Myelinated nerve fibers propagate electrical impulses (action potentials) not as a continuous wave of depolarization as the unmyelinated axons do, but in a saltatory fashion in which action potentials are regenerated in small patches of bare membrane called nodes of Ranvier.[97] We will discuss first the limitations imposed by the characteristics of this preparation on the electrical techniques used to record resting potentials, action potentials, and later in voltage clamping. As said above, essentially all the patch isolation techniques were derived from those developed for the node of Ranvier, and thus the natural node will be described rather extensively. Voltage clamping of the node of Ranvier has become a standard technique in which low-noise current records, fast settling times, and accurate membrane potential control can be obtained without the use of extremely sophisticated electronics. Although studies of the node of Ranvier began in order to see if the insights developed by Hodgkin and Huxley were valid for the node, this preparation has become so popular in the past ten years that many of the recent developments in electrophysiology have been made on this preparation.[97]

10.6.1.1. General Characteristics. The techniques for dissection and mounting of single myelinated axons from the frog and toad have been discussed extensively by Stämpfli and Hille[97] and will not be covered here. The design of the chamber used to mount the nerve fibers and to make electrical recordings from the node of Ranvier depends on the technique employed, and its characteristics are described in connection with each of the available methods.

In order to orient the reader to the technical requirements of the node of Ranvier as an electrophysiological preparation, we have included in Table I the typical electrical parameters of a frog's myelinated fiber. From Table I we see that the node represents a very small patch of excitable membrane (22 μm^2) with a very high resting resistance (40–80 MΩ).

10.6.1.2. Membrane Potential Measurement in a Node of Ranvier. We recall that the requirements of a good voltage clamp technique are that the potential measurement must be *accurate*, *fast*, sampled at an *isopotential patch of membrane*. We discuss now to what extent this has been achieved in myelinated nerve fibers.

A straightforward method for measuring transmembrane potential in a biological preparation is the use of micropipettes. However, as suggested by the work of Woodbury,[97a] they cannot be successfully used in the node of Ranvier.

[97] R. Stämpfli and B. Hille, *in* "Frog Neurobiology" (R. Llinas and W. Precht, eds.), Springer-Verlag, Berlin and New York, 1976.

[97a] J. W. Woodbury, *J. Cell. Comp. Physiol.* **39**, 323 (1952).

TABLE I. Electrical Characteristics of a Frog's Myelinated Fibers

Fiber diameter	14 μm
Thickness of myelin	2 μm
Distance between nodes	2 mm
Area of nodal membrane (not measured directly)	22 μm^2
Resistance per unit length of axis cylinder	140 MΩ/cm
Specific resistance of axoplasm	110 Ωcm
Capacity per unit length of myelin sheath	10–16 pF/cm
Capacity per unit area of myelin sheath	2.5–5 nF/cm^2
Resistance times unit area of myelin sheath	0.1–0.16 MΩ cm^2
Specific resistance of myelin sheath	500–800 MΩ cm^2
Capacity of node of Ranvier	0.6–1.5 pF
Resistance of resting node	40–80 MΩ
Action potential amplitude	116 mV
Resting potential	−71 mV
Peak inward current density	20 mA/cm^2

An alternative method for measuring the potentials in this preparation was introduced by Huxley and Stämpfli.[98] Figure 11a shows a shematic drawing of the preparation and their electronic arrangement. The rationale of the Huxley–Stämpfli method is that of a simple potentiometric recording. The membrane potential V_m of node 0 in Fig. 11b can be measured without attenuation if the current source H supplies current through the partition AB until the meter G shows no deflection, indicating no current flow across the resistance R_{BC}. Since node −1 is not contributing to the membrane potential (because it is depolarized by KCl), then $V_{AB} = V_m$. If there is current flowing through the external resistor R_{BC}, the potential at C does not represent V_m, but is an attenuated membrane potential value. If there is no current flow, though, $V_C = V_B = V_D = V_m$. Huxley and Stämpfli[98] were able to measure accurately the resting potential and the peak value of the action potential in nodes of *Rana esculenta* by setting the current at H manually by trial and error to a value which blocked current flow. Their method has been called *static potentiometric* since the zero-current condition was only met at specific points of the electrical cycle.[97]

In the experiments of Huxley and Stämpfli the gap BC, measuring approximately 600 μm, was filled with paraffin oil and had a resistance of about 10 MΩ. The resistance of the whole loop DCBAD was between 60 and 90 MΩ; the voltage drop across the gap BC is only a small fraction of V_m, and an action potential will seem very small because of this voltage dividing effect (attenuation) unless the potentiometric method is used. In order to record action potentials, this attenuation has to be reduced dramatically, and two approaches have been followed in order to achieve

[98] A. F. Huxley and R. Stämpfli, *J. Physiol. (London)* **112**, 476 (1951).

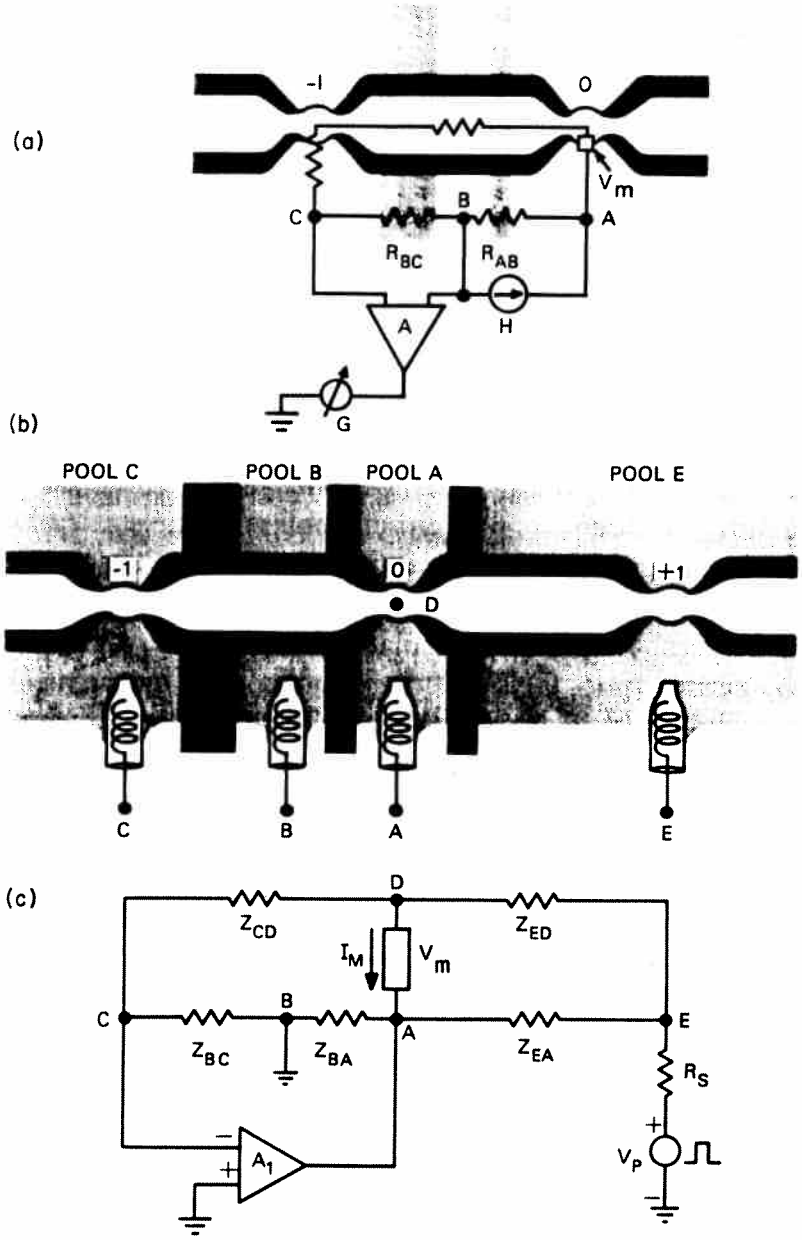

FIG. 11. Potentiometric methods of recording membrane potential. (a) Schematic diagram of the Huxley–Stämpfli[98] static potentiometric methods. Node 0 has a resting potential V_M and node -1 is depolarized by isotonic KCl. Shaded regions represent partitions. The BC partition is filled with paraffin oil and has a resistance of about 10 MΩ. The AB partition is a small trough with a resistance of about 20 KΩ. H is a current source, G is a galvanometer indicating the zero-current condition, and A is a differential amplifier measuring the voltage drop across R_{BC}. (b) Schematic diagram of Frankenhauser[81] dynamic potentiometric method. Node 0 has a resting potential V_M and nodes -1 and $+1$ are depolarized by isotonic KCl. Stippled regions represent petroleum jelly seals with resistance of about 5–10 MΩ. Important points are labeled and correspond to those in the circuit diagram shown in (c). (c) Equivalent circuit of Frankenhauser's method. The electrode impedance and balancing circuits are not considered; Z indicates generalized impedances as used in Section 10.A.1. They are drawn and described in the text as resistances for simplicity only. R_s is the output impedance of the stimulator (about 500 Ω). Amplifier A_1 is a high-input-impedance, wide-bandwidth amplifier. For complete discussion see text and Section 10.A.2.

this goal: (i) improved gap insulation and (ii) the dynamic potentiometric method.

10.6.1.2.1. GAP INSULATION. The resistance of the gap across which the potential is measured has to be made very high. In one method, Stämpfli[99] replaced the conductive solution in pool B of the Huxley–Stämpfli recording apparatus by deionized isotonic sucrose solution. In another method, Tasaki and Frank[100] eliminated the pool B and made a large air gap in the internodal region. With these methods the problem of attenuation has been largely reduced even though the use of an air gap, for example, requires very extensive drying of the preparation to obtain less than 10% attenuation. The disadvantages of gap insulation methods for voltage clamp techniques reside not only in the problem of the static or dc attenuation factors that violate our requirement of accuracy of potential measurement, but also in the dynamic attenuation factors introduced by stray capacitances. In the gap insulation techniques, the pool at which node − 1 is located (pool C) is effectively insulated from the measuring pool (pool A), which is usually grounded. This means that pool C is a very high-impedance pool with respect to ground and that any measurement of potential made there will be affected by stray capacitances to ground, slowing down the recording system. Action potentials at room and even low temperatures are fast processes that can be seriously distorted if the frequency response of the recording apparatus is below 5 kHz. With high-impedance gaps of the order of 100 MΩ, only 2 pF are necessary to cut the frequency response below 1 kHz. In these cases it is necessary to introduce negative-capacity compensation techniques or driven-shield techniques that introduce instability in the voltage clamp circuits and/or complicate the electronic circuitry.

10.6.1.2.2. POTENTIOMETRIC METHODS. We have already discussed the Huxley–Stämpfli method as a static-potentiometric method in which the action potential time course cannot be continuously displayed because the amount of current supplied by H is manually changed. Their method, though, did not require a very high gap resistance R_{BC} since the current source H was adjusted until no current flowed through the partition BC. From the diagram shown in Fig. 11a it can be seen that if the potential drop across R_{BC} is differentially measured by an amplifier that in the case of Huxley and Stämpfli was used to inject current into pool B in a negative feedback configuration, then the potential drop across R_{BC} will be *dynamically* maintained at zero. This condition has been successfully used by Derksen[101] to record action potentials potentiometrically. The method still has the

[99] R. Stämpfli, *Experientia* **10**, 508 (1954).
[100] I. Tasaki and K. Frank, *Am. J. Physiol.* **182**, 572 (1955).
[101] H. E. Derksen, *Acta Physiol. Pharmacol. Neerl.* **13**, 373 (1965).

limitation that there is a relatively high impedance between the voltage measuring circuit and ground. This limits the bandwidth of the recording system and negative-capacitance compensation is required to avoid attenuation of fast signals such as the action potential. A related but new method of potential measurement in the node of Ranvier that has overcome many of these difficulties has been designed by Frankenhauser.[81]

The schematic diagram of the experimental arrangement of Frankenhauser's Vaseline gap technique is shown in Fig. 11b, and the equivalent circuit is shown in Fig. 11c.† It can be seen in Fig. 11b that there are three nodes (-1, 0, and $+1$) involved in the circuit instead of the two nodes used in the Huxley–Stämpfli method. The third node (in pool E, Fig. 11b) is used to pass current and stimulate the preparation. The circuit equations of Frankenhauser's method can be deduced from Fig. 11c.

It was shown by Frankenhauser[81] [see Section 10.A.1, Eq. (10.A.1)] that the potential in pool A is given by:

$$V_A = -V_m A R_{BC}/[R_{BC}(A + 1) + R_{CD}], \tag{10.6.1}$$

where V_m is the membrane potential of the node, A is the gain of amplifier A_1, and R_{BC} and R_{CD} are the resistances between the respective points in the circuit diagram‡ (Fig. 11c). This result demonstrates the effectiveness of the potentiometric recording of V_m since from Eq. (10.6.1), when the open-loop gain of the amplifier A_1 becomes large, V_A approximates the membrane potential,

$$V_A = -V_m \qquad A \to \infty. \tag{10.6.2}$$

In this situation it can be seen that V_D and V_C are both equal to zero. This is the same as saying that V_C is virtual ground, and since B is at ground potential, no current can flow through R_{BC}, in which case, no current flows through the resistance R_{CD}, verifying that the recording of V_m is potentiometric. In fact, the effective loop resistance defined as $(V_A - V_C)/I_{CD}$ is very high, given approximately by

$$R_{loop} = R_{BC}(A + 1). \tag{10.6.3}$$

In the derivation of Eqs. (10.6.1)–(10.6.3), we did not consider any current drain at the input of the amplifier A_1, for which purpose a high-impedance amplifier has to be used. Field-effect-transistor input amplifiers are currently available with impedances of 10^{12}–$10^{13}\,\Omega$; this effectively prevents any

† In this diagram and the following ones, electrode potentials and balancing circuits are not included. In the actual implementation of the Frankenhauser method, a balancing circuit is required to cancel electrode potentials. If this balance potential is misadjusted, V_C will be different from zero; consequently, V_D will also deviate from zero potential, but in a larger proportion than V_C (for a normal node $V_D \approx 20V_C$, Hille[60].

‡ In Section 10.A.1 and in Figs. 11–13 the linear circuit elements are labeled as generalized impedances. For simplicity, we use the same resistance notation in the text.

significant current from leaking into the amplifier itself. (Frankenhauser[81] used a grid pentode that drained less than 10^{-11} A.) It is interesting to note that the point D inside the node is held at virtual ground by the amplifier A_1 and that the external solution at pool A is at $-V_m$, which is the inverse of the situation in conventional methods of recording membrane potential. In the three Vaseline gap techniques of Frankenhauser, node +1 (pool E) is used to stimulate node 0. Vaseline insulation is necessary to inject current into the fiber, preventing current leaks between pools E and A. It is clear, however, by inspection of Fig. 11c that in this case the membrane potential V_m would be shunted by the resistance given by the series combination $R_{ED} + R_{EA}$. This would produce current flow through the membrane, defeating the whole purpose of the potentiometric method unless the potential at pool E is forced to be close to zero, preventing current flow across the R_{ED} resistance. In the actual implementation of the Frankenhauser technique, a stimulator is connected between E and ground, providing a low-resistance pathway given by the output impedance of the unit. In this case current will circulate through R_{ED} only during the stimulus when V_E is made different from zero. Frankenhauser[81] pointed out this problem and used a 500-Ω-output impedance stimulator (R_s) to correct it. It is concluded, then, that the stimulator used in the Frankenhauser method should be a voltage rather than a current generator.

Probably the most important improvement of Frankenhauser's method of measuring the potential of the node of Ranvier over previous methods is the fact that pool C, a high-impedance pool, is electronically at virtual ground. This means that stray capacitances to ground would be insignificant alternative current pathways, thus improving the frequency response of the recording circuit without the need of negative-capacity compensation and other speeding-up techniques. Frankenhauser[81] reported a bandwidth for his apparatus of 30 kHz which seems satisfactory for most electrophysiological studies.

10.6.1.3. Voltage Clamp of the Node of Ranvier. Several arrangements to control the membrane potential in a single node of Ranvier have been reported.[102–108] Of these, the most commonly used today is that introduced by Dodge and Frankenhauser[105] with modifications described by Nonner[108]

[102] J. del Castillo, J. Y. Lettvin, W. S. McCulloch, and W. Pitts, *Nature (London)* **180**, 1290 (1957).

[103] B. Frankenhauser and A. Pearson, *Acta Physiol. Scand.* **42**, Suppl. 145, 45 (1957).

[104] I. Tasaki and A. F. Bak, *J. Neurophysiol.* **21**, 124 (1958).

[105] F. A. Dodge and B. Frankenhauser, *J. Physiol (London)* **143**, 76 (1958).

[106] F. A. Dodge and B. Frankenhauser, *J. Physiol. (London)* **148**, 188 (1959).

[107] C. Bergman and R. Stämpfli, *Helv. Physiol. Pharmacol. Acta* **24**, 247 (1966).

[108] W. Nonner, *Pfluegers Arch.* **309**, 176 (1969).

and Hille.[109] Del Castillo and Moore (see Moore and Cole[20]) cut the nerve fibers in pool E to be able to inject current more efficiently into the node 0. Nonner[108] included as standard in his methods the cut of the fiber at the internodes; Hille[109] also cut the fibers at the internodes, but used the Dodge–Frankenhauser electronic arrangement using two amplifiers for voltage clamping instead of one as described by Nonner.[108] Figure 12a shows Hille's[109] modification of the Dodge–Frankenhauser system. The circuit diagram of the Dodge–Frankenhauser voltage clamp is shown in Fig. 12b.

We have previously shown that if A (the voltage gain of amplifier A_1) is large, the following statements are approximately valid:

(a) $V_C = V_D = 0$,
(b) $V_A = -V_m$,
(c) no current flows in circuit ADCB; therefore, current injected through R_{ED} flows only through circuit EDA.

It is easy to see how Frankenhauser's potentiometric voltage measuring circuit can be used in a voltage clamp configuration if we connect a second amplifier A_2 in the circuit as shown in Figs. 12a and 12b. The following equation can be written when the second amplifier A_2 of gain A' is connected:

$$V_E = A'(V_+ - V_-) = A'(V_A + V_{com}).$$

From this equation it follows that $V_A = -V_{COM}$; since V_A is maintained at $-V_m$ by amplifier A_1,

$$V_m = V_{COM}.$$

The conclusion is that amplifier A_2 passes current through the membrane to keep $V_m = V_{COM}$. In order to calculate the value of the current I_m we can observe that point D is at zero potential, and since no current flows through DCB, then

$$V_E = I_m R_{ED}, \qquad I_m = V_E/R_{ED}.$$

In Section 10.A.1 a general derivation is presented with Laplace-transformed variables considering A and A' as functions of frequency. The above equations are only valid in the limiting case when A and $A' \to \infty$ for all frequencies.

One of the limitations of the Dodge–Frankenhauser voltage clamp is related to the attenuation factor. When we discussed Frankenhauser's potentiometric method for measuring potential from the node of Ranvier, we found that the loop resistance with amplifier gain A was $R_{BC}(A + 1)$

[109] B. Hille, *J. Gen. Physiol.* **58**, 599 (1971).

(a)

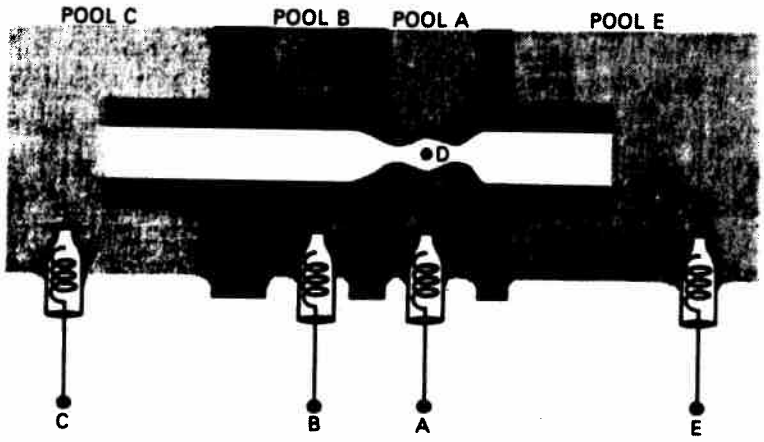
POOL C
POOL B
POOL A
POOL E
D
C
B
A
E

(b)

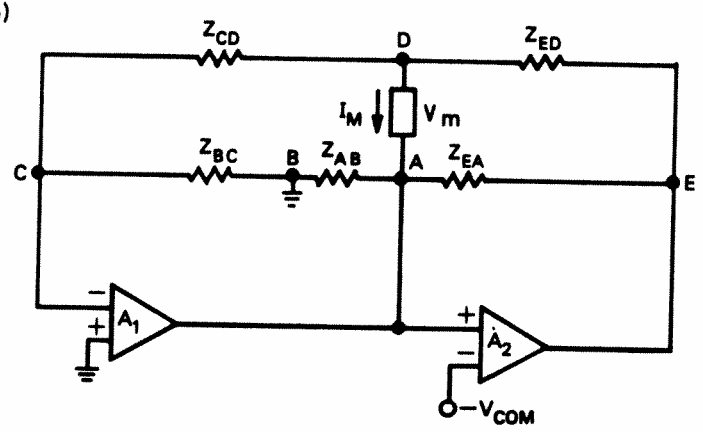
Z_{CD}
D
Z_{ED}
I_M
V_m
Z_{BC}
B
Z_{AB}
A
Z_{EA}
C
E
A_1
A_2
$-V_{COM}$

(c)

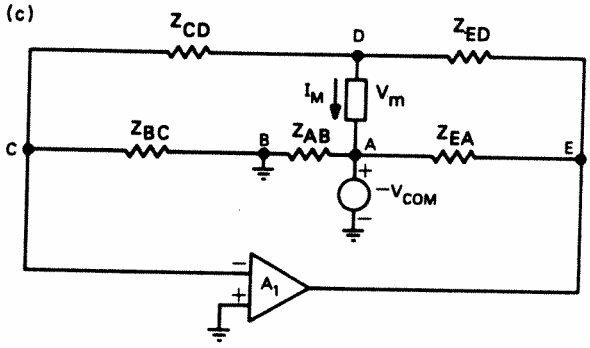
Z_{CD}
D
Z_{ED}
I_M
V_m
Z_{BC}
B
Z_{AB}
A
Z_{EA}
C
E
$-V_{COM}$
A_1

[Eq. (10.6.3)], which minimized the attenuation factor. A limitation in this method arises because pool B cannot be made wide enough to prevent the attenuation; a wide pool leads to a large phase lag in the potential recording system. This phase lag was acceptable for recording the membrane action potential but seriously limits the stability characteristics of the closed-loop configuration when the voltage clamp amplifier (A_2) is incorporated in the loop. A very simple rule defining the stability characteristics of a feedback control circuit is that the feedback should never become a positive feedback for gains larger than 1. Phase lags introduced by the loop network and the amplifier itself may transform the negative feedback into positive feedback if the signal frequency becomes higher than certain values. A phase lag of 90° between the input and output signals of a network is produced by each "pole" in a transfer function equation. A system with two poles, then, can produce a phase lag of 180°, and if such a network is in the feedback loop, the closed-loop system may become unstable for gains larger than 1. When the second amplifier (A_2) is added in order to voltage-clamp the preparation the situation becomes more critical. We can observe that the input signal to A_2 is V_A, which already has a phase lag introduced at least by the product $A(s)Z_{BC}(s)$. Amplifier A_2 will add at least another pole to the system, making necessary a careful analysis of the network closed-loop equations in order to

FIG. 12. Hille's modification of the Dodge–Frankenhauser[105] voltage clamp of the node of Ranvier and Nonner voltage clamp. (a) Schematic diagram: Myelinated fibers of about 16 μm internodal diameter and 1.5 mm internodal length are used. The nerve is mounted in an acrylic chamber in which the size of the pools is adjustable.[108] Four pools (shaded areas) are formed by laying three strings of Vaseline (black areas). The fiber is cut in pools E and C. Pools A and B contain Ringer's solution and pools E′ and C contain isotonic KCl or CsF solution. The sizes of the gaps are 500 (BC), 200 (AB), and 200 μm (EA); the sizes of the pools are 250 (pool B) and 150 μm (pool A). Seal resistances are about 5 MΩ. The electrical connections are made through 1 *M* KCl agar bridges to calomel electrodes to which the electronic equipment is connected. V_{COM} includes the pulse and holding potential. (b) Equivalent circuit of the method: Amplifier A_1 has gain $A(s)$ and amplifier A_2 has gain $A'(s)$. Amplifiers A_1 and A_2 need to be phase-lag compensated. Membrane current (I_M) is measured as V_E/Z_{ED} and membrane potential as $-V_A$. To measure the membrane potential under current-clamp conditions, amplifier A_2 is disconnected, and E is connected to a pulse generator to stimulate the preparation as shown in Fig. 11c. For details see text and Section 10.A.1. (c) Equivalent circuit of Nonner's method: Same as (b) except that only one amplifier is used to voltage-clamp the preparation. The voltage generator used to impose the membrane potential (V_{COM}) had an output impedance of 200 Ω and the feedback amplifier A_1 had high input impedance (100 MΩ, 7 pF), low bias current (10^{-12} A), and low output impedance (100 Ω) in addition to wide bandwidth and high amplification (up to 86 dB). The amplifier was compensated based on measurements of the open-loop characteristics of the circuit using the Nyquist stability criterion.[58] The membrane current is measured indirectly (V_E) and the membrane potential is measured as the negative of the potential at pool A. In order to measure the voltage in a current-clamp configuration, the output of amplifier A_1 has to be connected to A (instead of E), disconnecting the stimulator V_{COM}. V_M is measured as $-V_A$ under those conditions.

evaluate its stability. Such a study has been done by Nonner,[108] who introduced a new voltage clamp system for the node preparation.

Nonner's method represents an improvement of the Dodge–Frankenhauser method mainly in two respects: (i) the attenuation artifact was eliminated even though the size of pool B was made very small, and (ii) by studying carefully the loop impedances and eliminating one of the amplifiers of the loop, the frequency response of the voltage clamp could be increased to at least 10 kHz, which allows one to observe the rapid ionic conductance transients occurring at room temperature. A circuit diagram of Nonner's technique[108] is shown in Fig. 12c, and a general derivation of the circuit equations is presented in Section 10.A.1. The air gap included in his technique helped to eliminate the attenuation artifact described by Dodge and Frankenhauser (discussed above), probably because the leak through the Schwann cell space disappeared with the drying of a certain portion of the internode. To record membrane potential under current clamp condition, Nonner[108] used directly Frankenhauser's potentiometric method, but to voltage-clamp the nodal membrane he switched the output of the potentiometric amplifier from pool A (current clamp) to pool E (voltage clamp). The voltage clamp method is also based on the fact that C becomes virtual ground when the gain A of the amplifier is large. In that condition the current through R_{CD} is zero, and point D is also virtual ground. The potential at pool A becomes $-V_m$. If a low-impedance voltage source is used to set the value of V_A to $-V_{COM}$, it follows from the equations discussed in Section 10.A.1 that $V_m = V_{COM}$. In order to measure the membrane current I_m we demonstrate also in Section 10.A.1 that $I_m = V_E/R_{ED}$. It is interesting to observe that the final voltage clamp condition is achieved with Nonner's technique without several of the stability complications present by the use of two amplifiers in the Dodge–Frankenhauser technique. The second amplifier (A_2) of the latter technique is redundant in the voltage clamp situation; A_2 can be replaced by connecting the output of amplifier A_1 to E and adding a low-impedance source to set the value of V_A as Nonner did. The equations can be compared with the Dodge–Frankenhauser loop equations to verify that the elimination of one of the amplifiers simplifies the equations for the loop and thus makes easier the design of a fast and stable voltage clamp. For an analysis of the stability characteristics, it is possible to set values for the terms included in the loop equations and study system performance using the stability criteria commonly used in feedback control systems (see, for example, D'Azzo and Houpis[58] and Nyquist[110]). Nonner[108] analyzed his voltage clamp system extensively and the reader is referred to his paper for an explicit discussion.

[110] H. Nyquist, *Bell Syst. Tech. J.* (1932).

Instrumental and thermal noise associated with Nonner's voltage clamp technique were analyzed by Conti *et al.*[111] when they used this technique to measure Na current fluctuations in the node of Ranvier. They found that the background thermal noise contributions from the partitions and passive membrane patch may be reduced by increasing Z_{ED}, Z_{BC}, and membrane impedance Z_m, and by decreasing Z_{CD}. Besides, the amplifier's voltage (e_n^2) and current (i_n^2) input noise are multiplied by factors (containing the impedances Z_{ED}, Z_{BC}, Z_{CD}, and Z_m) that are minimized by the same procedure.

10.6.2. Vaseline-Gap Techniques in Single Muscle Fibers

Frankenhauser *et al.*[112] demonstrated that the principles involved in potentiometric recording of membrane potential at the node of Ranvier can be applied to single muscle fibers. The error in the potential measurement in this latter preparation is about 1% at low frequencies, but can reach about 10% at frequencies of 50 kHz. Since a 50-kHz bandwidth is adequate for most purposes, their method has been attractive enough to encourage muscle investigators to use it for voltage clamp studies. Moore[113] applied for the first time the potentiometric method for triple-Vaseline-gap voltage clamp studies in single muscle fibers.

A significant improvement on the three-Vaseline-gap voltage clamp, and on muscle voltage clamps in general resulted from the work of Hille and Campbell.[114] These authors applied the Dodge–Frankenhauser[105] techniques to short segments of muscle fibers cut at both ends instead of one end as Moore[113] did. They also cut the fibers in a solution of isotonic CsF, which helped to keep the cut ends unswollen and left the muscle membrane in pool B depolarized but with high resistance. The diagram and schematic circuit of the Hille–Campbell voltage clamp technique is shown in Fig. 13. The circuit equations for that configuration are developed in Section 10.A.1

In order to have a fast and stable voltage clamp circuit, Hille and Campbell[114] employed the discrete amplifiers previously used by Nonner[108] that can be externally compensated. The compensation network for amplifiers A_1 and A_2 in the Hille–Campbell voltage clamp can be calculated theoretically from the open-loop equations and/or determined by trial and error until the open-loop Bode plot has a rolloff of less than 20 dB/decade.

[111] F. Conti, B. Hille, B. Neumcke, W. Nonner, and R. Stämpfli, *J. Physiol. (London)* **262**, 699 (1976).

[112] B. Frankenhauser, B. D. Lindley, and R. S. Smith, *J. Physiol. (London)* **183**, 152 (1966).

[113] L. E. Moore, *J. Gen. Physiol.* **60**, 1 (1972).

[114] B. Hille and D. T. Campbell, *J. Gen. Physiol.* **67**, 265 (1976).

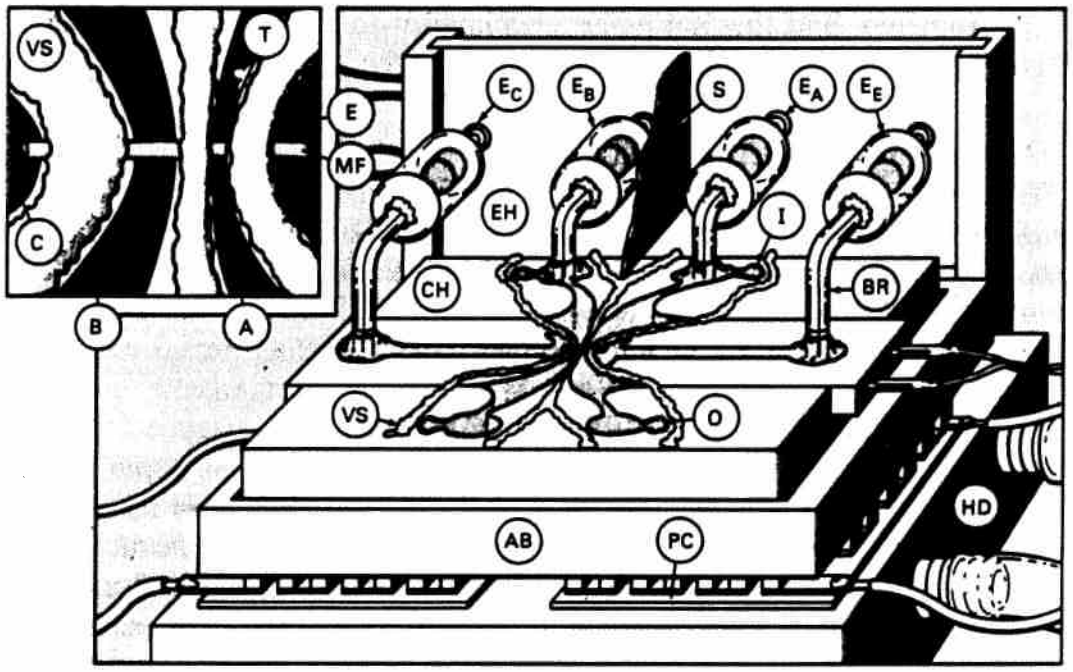

FIG. 13a. Voltage clamp of single muscle fibers with Vaseline-gap technique. Experimental chamber: The chamber (CH) is built of Lucite and rests on an aluminum block (AB) cooled by Peltier coolers (PC) connected to a feedback circuit to control the temperature measured by a thermistor (T) installed in pool A (see inset). HD is the heat dissipator for the Peltier coolers. The four electrodes (E_C, E_B, E_A, and E_E) are built with pellets of sintered Ag/AgCl in 1 *M* KCl connected to the chamber with agar bridges (BR) filled with 1 *M* KCl and containing a floating platinum wire to decrease the high-frequency impedance. The electrodes are mounted in an electrode holder (EH) that can be removed for storage of the electrodes. Pools are separated by Vaseline strings (VS), and solutions are changed by supplying solution at I and sucking it away at O. Inset: detail of a muscle fiber segment (MF) installed in the chamber. The pools are marked (A, B, C, E). VS are the Vaseline seals, and T is the thermistor.

The reason trial and error may be necessary is that the phase lags introduced by the preparation arise from a cable structure and not a lumped *RC* network.

One of the limitations of the Vaseline-gap voltage clamp (common to any voltage clamp system in which the length constant of the preparation is not modified by impalement with an axial wire) is that the membrane current is collected from a patch of membrane of finite length, while the potential control is restricted to a membrane ring at the AB partition. We shall discuss this problem extensively below in Section 10.6.4 and Section 10.A.2 as a general limitation of gap voltage clamps with special reference to a discussion by Hille and Campbell[114] of the muscle-fiber voltage clamp.

The Hille–Campbell technique for muscle-fibers voltage clamps has been used successfully to record sodium channel gating currents and excitation–contraction (EC) coupling charge movements.[115] It has further been

[115] J. Vergara and M. Cahalan, *Biophys. J.* **21**, 167a (1978).

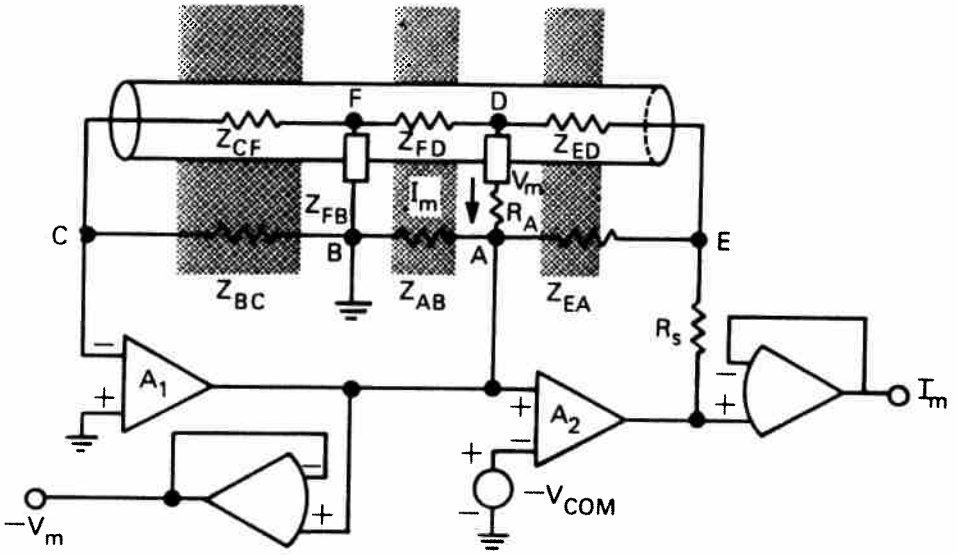

FIG. 13b. Voltage clamp of single muscle fibers with Vaseline-gap technique. Equivalent circuit: The diagram is similar to that of Fig. 12b (the Dodge–Frankenhauser voltage clamp). In this case there is an additional impedance Z_{FB} that represents the membrane patch in pool B. A resistance in series with the output of amplifier A_2 (R_s) is included to measure the total current I_E, but is selected of a small value (1 KΩ) and is not included in the derivation found in Section 10.A.1. Another resistance that has not been included in the derivations of Section 10.A.1 is a series resistance R_A with the membrane in pool A that should be compensated for by positive feedback.[114] It can be readily incorporated by replacing V_m by $V_m + I_m R_A$ in Eq. (10.A.14) of Section 10.A.1. A discussion of series resistance compensation is presented in Section 10.3.5.3.

used to study optical events related to the EC coupling in muscle fiber.[116,117] Vergara *et al.*[116] report a modification of the Dodge–Frankenhauser[105] chamber to include an optical fiber in pool A to illuminate the muscle fiber and verified that it can still be used for voltage clamp experiments. They also improved the Hille–Campbell technique in three aspects.

(1) The fibers were cut in relaxing solutions containing K-Aspartate instead of CsF or KF. Under these conditions the fibers are able to contract in the region of pool A (and only there) when they are depolarized. The movement associated with the depolarization is blocked by adding 2–4 mM EGTA in pool E and C and waiting about 20 min for diffusion.

(2) The fibers were depolarized for the first time, after dissection, in a high-K solution keeping the fibers stretched, thus preventing the over-shortening that occurs when they are depolarized without being held. Under those conditions the fiber contracts and relaxes as described by Hodgkin and Horowicz.[118] The sarcomere length of the fibers, mounted after

[116] J. Vergara, F. Bezanilla, and B. M. Salzberg, *J. Gen. Physiol.* **72**, 775 (1978).
[117] P. Palade, *Biophys. J.* **25**, 142a (1979).
[118] A. L. Hodgkin and P. Horowicz, *J. Physiol.* (*London*) **153**, 386 (1960).

this precaution is taken, is about $2.4 \pm 0.2\,\mu m$[116] instead of $1.6 \pm 0.2\,\mu m$ reported by Hille and Campbell.[114]

(3) When the fibers were treated with TTX, normal-looking delayed K currents were described, whereas one of the major difficulties in the Hille–Campbell[114] report was that they were not able to record normal-looking K currents.

It should be pointed out finally that the fact that both ends of the fibers are cut means that both can be used to diffuse substances to the fiber interior and eventually replace the normal ionic content of the sarcoplasm. Undoubtedly, a good blockage of the K current can be obtained in this preparation by soaking the cut ends in a solution containing CsF.[114]

The Hille–Campbell technique and subsequent modifications of it constitute a reasonably accurate voltage clamp system for muscle fibers. We discuss below in Section 10.6.4 the limitations of gap isolation voltage clamps and give there error criteria for judgment of the longitudinal dispersion of the membrane potential of the fiber along the control pool. One conclusion to be drawn from that analysis is that if the gap is made small with respect to the radius of the fiber and the conductance of the membrane does not become too large, the membrane in the gap can be considered almost isopotential in the longitudinal direction.

10.6.3. Sucrose-Gap Methods

Stämpfli[99] introduced the use of deionized sucrose to increase the impedance of the recording gap. This technique was extended to voltage clamp by Julian *et al.*[119,120] for nonmyelinated giant axons of the lobster and by Moore *et al.*[121] for the squid giant axon.

Two sucrose gaps and three pools (two lateral and one central) are defined for voltage-clamping a cylindrical cell. Julian *et al.*[119,120] called the lateral pools *I* pool (at which current was injected to the fiber) and *V* pool (at which voltage was recorded). The central pool was used for current recording and was kept at virtual ground by a current-to-voltage converter. The length of their sucrose gaps was about $600\,\mu m$, and the central pool could be made as narrow as $50\,\mu m$. The gap resistances were at least $25\,M\Omega$, and under these conditions the potential measurements are accurate with less than 5% error. The sucrose-gap technique has the problem that there is a 20–60 mV hyperpolarization in the recorded potential[120] that has been suggested to arise from a liquid junction potential between sucrose and

[119] F. J. Julian, J. W. Moore, and D. E. Goldman, *J. Gen. Physiol.* **45**, 1217 (1962).
[120] F. J. Julian, J. W. Moore, and D. E. Goldman, *J. Gen. Physiol.* **45**, 1195 (1962).
[121] J. W. Moore, T. Narahashi, and W. Ulbricht, *J. Physiol.* (*London*) **172**, 163 (1964).

sea water.[122] Despite this problem, the currents recorded with the sucrose-gap technique in giant axon suggest that good potential control is achieved provided that the central gap length is not longer than the fiber diameter (see discussion below).

The sucrose-gap technique described by Julian *et al.*[119,120] has been used almost without modification in skeletal muscle fibers by Nakajima and Bastian.[123] These authors found, though, that the Julian–Moore–Goldman techniques could not be used directly with single muscle fibers of the frog but could be applied to *Xenopus* muscle fibers. Nakajima and Bastian[123] also found, as expected and discussed above, that an important bandwidth limitation (in the voltage clamp) is induced by stray capacitances to ground; their potential recording pool V is a high-impedance pool.

A modification of the double-sucrose-gap technique was made by Ildefonse and Rougier[124] to voltage-clamp single muscle fibers of the frog. Their system is not only a sucrose-gap technique but also uses Vaseline and sucrose.

Recently, Duval and Leoty[125] have used a double-sucrose-gap technique in mammalian muscle fibers in which they cut the ends of the fibers, thus improving the performance of the voltage clamp. Duval and Leoty[125] also measured the potential in the test gap lengthwise with a microelectrode, verifying that there was a partial lack of longitudinal control. They decided that gap lengths of 100 μm for fibers of 50–70 μm were safe values to prevent this lack of control. In the next section we discuss this problem extensively.

10.6.4. Errors Introduced by the Finite Length of the Gap

The measurement of current in the gap voltage clamp will only be exact if the length of the gap is made infinitesimally small. We consider in this section the errors introduced by making the gap of finite length.

This problem has been considered theoretically by Cole (Ref. 7, p. 418) and is analyzed in detail in Section 10.A.2. We show there that in most experimental situations the core-conductor approximation is valid.† We give formulas to calculate both the maximum error in the voltage at the EA

[122] M. P. Blaustein and D. E. Goldman, *Biophys. J.* **6**, 453 (1966).
[123] S. Nakajima and J. Bastian, *J. Gen. Physiol.* **63**, 235 (1974).
[124] M. Ildefonse and O. Rougier, *J. Physiol. (London)* **222**, 373 (1972).
[125] A. Duval and C. Leoty, *J. Physiol (London)* **278**, 403 (1978).

† Our three-dimensional model in Section 10.A.2 does not include a T-system network; consequently, the core-conductor cable model may not be a good description of a muscle fiber in a gap.

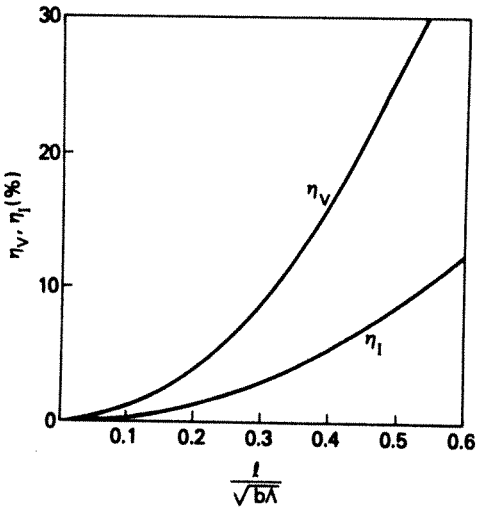

FIG. 14. Errors produced by finite gap length: Maximum error in membrane voltage η_V and in membrane current η_I produced by the length of the gap as computed by Eq. (10.A.28) and (10.A.29) derived from the core-conductor model in Section 10.A.2.

partition with respect to the controlled voltage and the error in the measured current with respect to the current across a controlled patch of membrane. These errors are plotted in Fig. 14 as a function of a single parameter $l/\sqrt{b\Lambda}$, in which l is the length of the gap at pool A, b is the fiber diameter, and Λ is the generalized space constant defined in Section 10.A.2. The experimentalist can estimate from Fig. 14 the maximum gap length that assures him voltage and current control, within a selected tolerance, when the fiber parameters b and Λ are known. Hille and Campbell[114] calculated the longitudinal variations of the potential inside the fiber assuming that the membrane current is constant and that the fiber in pool A can be considered as a semi-infinite cable. They derived

$$V(l) = I_M R_i l^2/A. \tag{10.6.4}$$

In the potentiometric method, the internal potential $V_D(z)$ can be defined as

$$V_D(z) = V(z) - V_0,$$

in which $V(z)$ is the membrane potential as a function of the distance from the AB partition and V_0 is the potential at the AB partition ($z = 0$). If we make this change of variable in Eq. (10.A.27) of Section 10.A.2, we obtain (see also Cole[7])

$$V_D(z) = V_0(\cosh(z\sqrt{2}/\sqrt{b\Lambda}) - 1). \tag{10.6.5}$$

A first-order approximation of the Taylor-series expansion of Eq. (10.6.5) evaluated at $z = l$ gives the Hille–Campbell result [Eq. (10.6.4)] provided

that the membrane current $I_M = V_0/R_m$ is constant over the entire length of the gap. It is interesting to observe in Fig. 14, though, that only at $l/\sqrt{b\Lambda}$ smaller than 0.05 can the membrane current be assumed constant, but at larger and still realistic values of $l/\sqrt{b\Lambda}$ (for an active membrane for example) this approximation no longer holds and the exact formula should be used. Within the restrictions imposed by the first-order approximation, Hille and Campbell[114] showed that $V_D(l)$ can be roughly estimated from the potential at pool E (V_E) by the formula

$$V_D(l) = V_E\, l/(l + 2k),$$

in which k is the length of the fiber segment from $z = l$ to the cut end at pool E. An exact formula relating $V_D(l)$ and V_E can be derived from Eq. (10.6.5) and other equations for the core-conductor model included in Section 10.A.1. The result

$$V_D(l) = V_E \frac{\cosh(l\sqrt{2}/\sqrt{b\Lambda}) - 1}{\cosh(l\sqrt{2}/\sqrt{b\Lambda}) + (k\sqrt{2}/\sqrt{b\Lambda})\sinh(l\sqrt{2}/\sqrt{b\Lambda}) - 1}$$

shows that, in the exact case, it is necessary to know the membrane parameters to estimate $V_D(l)$ as a function of V_E. The above equations may give the wrong impression that the potential $V_D(l)$ diminishes as k is made larger. This is not the case because the feedback amplifier (A_2) makes V_E larger if k increases, compensating for the change. The deviations of $V_D(l)$ are only functions of the error η_V in Fig. 14 and the imposed potential V_0.

The error criteria developed above can be used to roughly estimate the errors in voltage-clamping an active membrane. For example, when the K conductance increases upon depolarization Λ decreases, and if the current has reached a steady state (that is, when there is no K inactivation), a fairly good estimate of the errors in the records can be made from Fig. 14. In a non-steady-state situation Fig. 14 may still be used to obtain a rough estimate of the errors. For the case of negative conductance we have included in Section 10.A.2 Eqs. (10.A.31) and (10.A.32) to estimate η_V^a and η_I^a, respectively. It can be noticed that η_V^a and η_I^a in this case have opposite signs with respect to those calculated in the positive conductance case. Numerical computations with Eqs. (10.A.31) and (10.A.32) show that for values of $l/\sqrt{b\Lambda}$ in the range used in Fig. 14, η_V^a and η_I^a do not differ significantly, in absolute value, from η_V and η_I. These equations could be used in the steady state for cases in which Na inactivation is absent, but care should be exercised in using them when normal sodium conductance is present. For both positive and negative conductances in the non-steady-state situation, a better estimation of the errors can be obtained with numerical

computations of the cable equations using the Hodgkin and Huxley equations. This has been done for the sucrose gap case by Moore *et al.*[126,127]

10.7. Concluding Remarks

The concept that all cells are bounded by a superficial layer with very special properties was derived from measurements of electrical and osmotic properties. These cell membranes are highly permeable to water and to lipid soluble substances, and they transport ions, sugars, and amino acids up and down electrochemical gradients. In this article we have been concerned with certain techniques which are used to study the electrical properties of some cell membranes which are excitable, i.e., they respond to electrical or chemical stimuli and produce electrical effects. In order to study these electrical properties it is necessary to measure or control the voltage across and the current through the membrane over an area in which they are relatively uniform. This has been done most successfully with the giant axon of the squid, the node of Ranvier in myelinated axons, and by the development of gap techniques and patch isolation with external electrodes. Some very good work has been done using microelectrodes in both cylindrical and spheroidal cells, but the high resistance of such electrodes and problems of uniformity make quantitative studies difficult.

Much of this paper would be relevant to attempts to control current (current clamp), but the voltage clamp is emphasized because it is the natural quantity to control in a system with large capacitance and voltage-dependent elements.

10.A. Appendix

10.A.1. Circuit Equations of Vaseline-Gap Voltage Clamp

The purpose of this section is to develop the circuit equations of the potentiometric method of Frankenhauser, and three commonly used voltage clamp systems: (i) the Dodge–Frankenhauser voltage clamp of a myelinated-fiber node of Ranvier, (ii) the Nonner voltage clamp of a node of Ranvier, and (iii) the Hille and Campbell voltage clamp of a skeletal muscle fiber. The equations developed here can be adapted to modifications of these methods and we think they will help in understanding the basic

[126] J. W. Moore, F. Ramon, and R. W. Joyner, *Biophys. J.* **15**, 11 (1975).
[127] J. W. Moore, F. Ramon, and R. W. Joyner, *Biophys. J.* **15**, 25 (1975).

principles involved in their application. Voltage and currents are Laplace-transform variables, and the circuit elements are defined as generalized impedances Z_{xy} that may behave as pure resistors or a combination of linear elements. The potential at a point W of the circuit is called v_W. The transformed membrane potential and current are called v_m and i_m, respectively. The diagrams shown in Figs. 11–13 are used in the derivation of the circuit equations. Neither potentials associated with the electrodes nor balancing potentials will be considered here for two reasons: (i) the resulting equations are simpler, and (ii) every electrode potential should be balanced electronically to reach the configuration analyzed in the circuit diagrams that corresponds to the ideal case.

10.A.1.1. **Potentiometric Method of Frankenhauser.** The experimental arrangement and circuit diagrams are shown in Fig. 11c with $V_p = 0$. Using elementary circuit analysis and the relation

$$v_A = -Av_C,$$

we find

$$v_A = -v_m AZ_{BC}/(Z_{BC}(A + 1) + Z_{CD}) \tag{10.A.1}$$

and

$$i_m = -v_m(1 + K)/[Z_{BC}(A + 1) + Z_{CD}], \tag{10.A.2}$$

with

$$K = [(Z_{BC} + Z_{CD})(R_S + Z_{EA}) + AR_S Z_{BC}]/[R_S(Z_{EA} + Z_{ED}) + Z_{ED}Z_{EA}]. \tag{10.A.3}$$

In order to record the actual membrane potential without attenuation, i_m must be zero; this condition is only met when both $A \to \infty$ and $R_s \to 0$.

In practice when $A \to \infty$ we get, for R_S small,

$$i_m \to -v_m R_s/Z_{EA}Z_{ED}, \tag{10.A.4}$$

from which we can estimate how large R_s can be to keep i_m under a specified tolerance. For the node of Ranvier $R_s \approx i_m/v_m \times 10^{14}\,\Omega$. To drain less than 10^{-11} A from the node at $V_m \approx 100$ mV, $R_s = 10\,k\Omega$. In the case of the potentiometric method applied to muscle fibers, Z_{ED} is at least 100 times smaller than in myelinated nerve fibers and one can allow a maximum current drain from the membrane patch of about 10^{-10} A. This requires a resistance R_s of at most 1 kΩ.

10.A.1.2. Dodge–Frankenhauser Voltage Clamp of the Node of Ranvier. We consider the experimental arrangements and circuit diagrams shown in Figs. 12a and 12b, respectively. The final equations will contain the terms A and A', but only after the final derivation is made will the limits A and $A' \to \infty$ be taken. Ideally, A and A' are complex gains of the form $A(s) = A_0/(1 + s\tau)$, and the reader can use the equations derived here making that replacement to study the performance of his particular voltage clamp giving the appropriate form to every impedance element as well. In this case, we can analyze the circuit equations with the following equations for the amplifier configurations:

$$v_E = A'(v_A + v_{COM}) \tag{10.A.5}$$

$$v_A = -Av_C. \tag{10.A.6}$$

We obtain for v_m the following equation:

$$v_m = (v_{COM}A' - i_m Z_{ED}) \times [Z_{BC}(A + 1) + Z_{CD}]/[(Z_{BC} + Z_{CD} + Z_{ED}) + AA'Z_{BC}]. \tag{10.A.7}$$

For stability analysis of the type described earlier it is necessary to compute v_m/v_{COM} which can readily be obtained from Eq. (10.A.7) and to assume a linear membrane impedance to relate i_m and v_m. Thus i_m is given by

$$i_m = \{v_E[AA'Z_{BC} + (Z_{BC} + Z_{CD} + Z_{ED})] - A'v_{COM}(Z_{BC} + Z_{CD} + Z_{ED})\}/AA'Z_{ED}Z_{BC}. \tag{10.A.8}$$

If we take the limits $A \to \infty$ and $A' \to \infty$ in Eqs. (10.A.7) and (10.A.8) we obtain respectively

$$v_m = v_{COM} \tag{10.A.9}$$

and

$$i_m = v_E/Z_{ED}. \tag{10.A.10}$$

Equations (10.A.9) and (10.A.10) have always been considered the fundamental equations of the Dodge–Frankenhauser voltage clamp, but it should be kept in mind that Eqs. (10.A.7) and (10.A.8) are the more general equations because they consider A and A' finite and frequency dependent.

10.A.1.3. Nonner's Voltage Clamp. We shall follow the same scheme as in part (a) but the circuit equations will be solved for the diagram of Fig. 12c. The gain of amplifier A_1 is connected in such a way that

$$v_E = -Av_C \tag{10.A.11}$$

We can calculate v_m:

$$v_m = v_{COM} - i_m Z_{ED}(Z_{BC} + Z_{CD})/[(A + 1)Z_{BC} + Z_{CD} + Z_{ED}] \tag{10.A.12}$$

and

$$i_m = v_E[1/Z_{ED} - (Z_{CD} + Z_{BC} + Z_{ED})/AZ_{BC}Z_{ED}]. \tag{10.A.13}$$

If we take the limit $A \to \infty$, we get Eqs. (10.A.9) and (10.A.10) derived for the Dodge–Frankenhauser voltage clamp. It can be observed though that in Nonner's clamp, the general expressions for V_m and I_m are simpler than in the Dodge and Frankenhauser method. Because a single amplifier is used in the voltage clamp circuit the product of AA' present in Eqs. (10.A.7) and (10.A.8) does not appear in Eqs. (10.A.12) and (10.A.13).

10.A.1.4. Hille–Campbell Voltage Clamp of Single Muscle Fibers. The difference between the Hille–Campbell and Dodge–Frankenhauser methods is that in the former there is a patch of membrane in pool B not existing in the latter. This is shown in Fig. 13b as the impedance Z_{FB}. This term slightly changes the equations derived in part (b), giving

$$v_m = (v_{COM} A' - i_m Z_{ED})\alpha/\beta, \tag{10.A.14}$$

with

$$\alpha = Z_{BC}Z_{FB}(A + 1) + Z_{FD}(Z_{BC} + Z_{CD}) + Z_{CD}Z_{FB}$$

and

$$\beta = Z_{ED}(Z_{FB} + Z_{BC} + Z_{CF}) + (Z_{FB} + Z_{FD})(Z_{CD} + Z_{BC}) + AA'Z_{BC}Z_{FB}.$$

If we take the limit $Z_{FB} \to \infty$ in α and β, Eq. (10.A.14) becomes identical to Eq. (10.A.7). The equation for i_m is

$$i_m = v_E\beta/(AA'Z_{ED}Z_{BC}Z_{FB}) - v_{COM}[\beta/AZ_{BC}Z_{AB}Z_{ED}) - A'/Z_{ED}]. \tag{10.A.15}$$

If we take the limits $A \to \infty$ and $A' \to \infty$ we get Eqs. (10.A.9) and (10.A.10), which are then common for the three voltage clamp techniques discussed in this section. It should be noted that in Eqs. (10.A.14) and (10.A.15) the gain A of amplifier A_1 appears always multiplied by the impedance term $Z_{FB}Z_{BC}$ (e.g., $AZ_{FB}Z_{BC}$) instead of Z_{BC} as is the case for the node of Ranvier. This difference is important in designing a compensating network for stabilization of the voltage clamp of muscle fibers.

10.A.2. Potential Distribution for a Fiber in a Gap Voltage Clamp

In this section we first consider models that describe the membrane potential distribution at the control pool (pool A) in nonmyelinated fibers voltage clamped using a Vaseline- (or sucrose-) gap technique. We then study the influence of the gap length and fiber characteristics (space constant and diameter) on the accuracy of the voltage control and current measurements when the Vaseline- (or sucrose-) gap voltage clamp is used.

The first model used is a three-dimensional cylinder extending from partition AB ($z = 0$) to partition EA ($z = l$) in the case of a Vaseline-gap arrangement.

The potential $V(r, z)$ anywhere in the fiber can be obtained by solving the Laplace equation in cylindrical coordinates:

$$\frac{\partial^2 V}{\partial r^2} + \frac{1}{r}\frac{\partial V}{\partial r} + \frac{\partial^2 V}{\partial z^2} = 0, \tag{10.A.16}$$

where r is the radial coordinate from the axis of the cylinder and z is the longitudinal coordinate along the axis. There is no circular dependence because there is circular symmetry imposed by the following boundary conditions at the ends:

$$\partial V/\partial z = 0, \qquad z = 0, \tag{10.A.17}$$

$$\partial V/\partial z = R_i I_I, \qquad z = l, \tag{10.A.18}$$

where R_i is the internal resistivity (in Ω cm) and I_I is the density of current (in A/cm^2) injected at pool E which has no radial or angular dependence.

The membrane boundary condition is given by

$$\frac{1}{R_i}\frac{\partial V}{\partial r} + \frac{V}{R_m} = 0, \qquad r = b, \tag{10.A.19}$$

where we have assumed that the potential distribution has reached a steady state and that the external solution is isopotential at a potential zero.† R_m is the membrane resistance (in Ω cm^2) and b is the fiber radius.

---

† The condition of external potential equal to zero has been used to simplify the mathematical treatment and is directly applicable to the case of sucrose gap when using electrometric potential measurement. When using potentiometric potential measurement the *internal* potential is made virtual ground (as in the Dodge–Frankenhauser or Nonner methods; to use this treatment the internal potential $V_D(z, r)$ can be calculated as $V_D(z, r) = V(z, r) - V_0$.

We solved this boundary value problem applying the Hankel transform with the kernel (Özisik,[128] p. 135)

$$\sqrt{2}J_0(\beta_m r)/\{b[(R_i/R_m\beta_m)^2 + 1]^{1/2}J_0(\beta_m b)\},$$

where J_0 is the Bessel function of zeroth order and β_m are the roots of the equation

$$\beta J_1(\beta b) - \Lambda^{-1}J_0(\beta b) = 0,$$

where J_1 is the Bessel function of order one and Λ is the generalized space constant (see, e.g., Eisenberg and Johnson[75]) given by

$$\Lambda = R_m/R_i.$$

The resultant transformed ordinary differential equation

$$-\beta_m^2 \bar{V} + d^2\bar{V}/dz^2 = 0,$$

in which $\bar{V}$ indicates the Hankel transform of $V(r, z)$, was integrated, giving

$$\bar{V} = (\bar{I}_1 R_i/\beta_m)[\cosh(\beta_m z)/\sinh(\beta_m l)], \tag{10.A.20}$$

in which $\bar{I}_1$ is the Hankel transform of I_1. The potential $V(r, z)$ can be obtained by inversion of Eq. (10.A.20) (Ref. 128, p. 135), giving

$$V(r, z) = 2I_1 R_i b \sum_{m=1}^{m=\infty} \frac{J_1(\beta_m b)J_0(\beta_m r)\cosh(\beta_m z)}{J_0^2(\beta_m b)[(b/\Lambda)^2 + b^2\beta_m^2]\sinh(\beta_m l)}. \tag{10.A.21}$$

The membrane potential $V(b, z)$ is given by

$$V(b, z) = 2I_1 R_i \sum_{m=1}^{m=\infty} \frac{b/\Lambda}{\beta_m[(b/\Lambda)^2 + (b\beta_m)^2]} \frac{\cosh(\beta_m z)}{\sinh(\beta_m l)}. \tag{10.A.22}$$

As a second model[7] we consider the simple core conductor (see, e.g., Taylor[5]),

$$d^2V/dz^2 = 2V/b\Lambda \tag{10.A.23}$$

with the boundary conditions

$$dV/dz = 0, \quad z = 0; \quad dV/dz = I_1 R_i, \quad z = l. \tag{10.A.24}$$

The solution is

$$V(z) = I_1 R_i \sqrt{\tfrac{1}{2}b\Lambda}\, \frac{\cosh(z\sqrt{2/b\Lambda})}{\sinh(l\sqrt{2/b\Lambda})}. \tag{10.A.25}$$

[128] M. N. Özisik, "Boundary Value Problems of Heat Conduction." International Textbook Co., Scranton, Pennsylvania, 1968.

It can be demonstrated algebraically that when b/Λ is very small, Eq. (10.A.22) becomes Eq. (10.A.25). We have numerically computed and compared the results of Eqs. (10.A.22) and (10.A.25) and found that the core-conductor model [Eq. (10.A.22)] does not deviate more than 3% from the three-dimensional model [Eq. (10.A.25)], provided that two conditions are met simultaneously: (i) $b/\Lambda < 0.1$ and (ii) $l/b < 5$. These conditions are fulfilled in most experimental cases; therefore, we shall discuss the accuracy of the gap voltage clamp only considering the simpler case of the core-conductor model.

From Eq. (10.A.25) we can see that the membrane potential at $z = 0$, defined as V_0, is equal to

$$V_0 = I_I R_i \sqrt{\tfrac{1}{2} b\Lambda} / \sinh(l\sqrt{2/b\Lambda}). \tag{10.A.26}$$

The voltage clamp circuit is imposing V_0 at $z = 0$ and the potential as a function of the longitudinal parameter is then

$$V(z) = V_0 \cosh(z\sqrt{2/b\Lambda}). \tag{10.A.27}$$

This equation allows us to quantify the deviation of the membrane potential from the controlled potential V_0, being maximal at $z = l$. We can estimate this maximal deviation of the membrane potential (given as percentage error, η_V) as a function of the gap length l, the fiber diameter b, and the space constant Λ. This is given by

$$\eta_V(\%) = [(V(l) - V_0)/V_0] \times 100;$$

then,

$$\eta_V = 100[\cosh(l\sqrt{2/b\Lambda}) - 1]; \tag{10.A.28}$$

η_V has been plotted as a function of $l/\sqrt{b\Lambda}$ in Fig. 14. We can also estimate the deviation of the measured current from the current circulating at a controlled membrane patch ($z = 0$). At this point the membrane current density is given by

$$I_0 = V_0/R_m.$$

The measured membrane current density is experimentally defined as

$$I_m = I_I(\pi b^2)/2\pi bl = I_I b/2l.$$

Now we can define the percentage error in the current (η_I) as

$$\eta_I = [(I_m - I_0)/I_0] \times 100,$$

and replacing in Eq. (10.A.26),

$$\eta_I = 100 \frac{\sinh(l\sqrt{2/b\Lambda})}{l\sqrt{2/b\Lambda}}; \tag{10.A.29}$$

η_I is plotted as a function of $l/\sqrt{b\Lambda}$ in Fig. 14.

The above discussion is valid for steady-state positive membrane conductance. In order to roughly estimate the error during the activation of a negative conductance[7] we may use the same derivation and replace, in Eq. (10.A.25), Λ by Λ_a, defined as

$$\Lambda_a = -R_m/R_i.$$

When this replacement is done we obtain

$$V(z) = I_I R_i \sqrt{\tfrac{1}{2}b\Lambda_a} \frac{\cos(z\sqrt{2/b\Lambda_a})}{\sin(l\sqrt{2/b\Lambda_a})}. \tag{10.A.30}$$

The errors η_V^a and η_I^a can be calculated in an equivalent way as done above:

$$\eta_V^a = 100[\cos(l\sqrt{2b\Lambda_a}) - 1], \tag{10.A.31}$$

$$\eta_I^a = 100[\sin(l\sqrt{2b\Lambda_a})]/l\sqrt{2b\Lambda_a}. \tag{10.A.32}$$

Acknowledgments

We thank Dr. Richard FitzHugh for checking the derivation of the expression for the differential electrodes. This work was supported by UPHS AM25201.